J. Fluid Mech. (1995), *vol.* 292, *pp.* 111–152

A rapid-pressure covariance representation consistent with the Taylor–Proudman theorem materially frame indifferent in the two-dimensional limit

By J. R. RISTORCELLI[1], J. L. LUMLEY[2] AND R. ABID[3]

[1] Institute for Computer Applications in Science and Engineering, NASA Langley Research Center, Hampton, VA 23681, USA

[2] Sibley School of Mechanical and Aerospace Engineering, Cornell University, Ithaca, NY 14850, USA

[3] High Technology Corporation, NASA Langley Research Center, Hampton, VA 23681, USA

(Received 18 January 1994 and in revised form 3 January 1995)

A nonlinear variable-coefficient representation for the rapid-pressure covariance appearing in the Reynolds stress and heat-flux equations, consistent with the Taylor–Proudman theorem, is presented. The representation ensures that the modelled second-order equations are frame indifferent with respect to rotation in a number of different flows for which such an invariance is required. The model coefficients are functions of the state of the turbulence; they are valid for all states of a mechanical turbulence, attaining their limiting values only when the limit state is achieved. This is accomplished by a special ansatz that is used to obtain – analytically – the coefficients valid away from the realizability limit. Unlike other rapid-pressure representations in which extreme states are used to set model constants, here the coefficients are variable functions asymptotically consisted with – not fixed by – the limit states of the turbulence field. The mathematical principles invoked do not specify all the coefficients in the model; undetermined coefficients appear as free parameters which are used to ensure that the representation is asymptotically consistent with an experimentally determined equilibrium state of homogeneous sheared turbulence. This is done by ensuring that the modelled evolution equations have the same fixed points as those obtained from numerical and laboratory experiments for the homogeneous shear. Results of computations of homogeneous shear, with rotation and with curvature, are shown. Results are better, in a wide class of planar flows for which the model has not been calibrated, than those of other nonlinear models.

1. Introduction

Most turbulence models are devised for use in inertial coordinate systems. *Ad hoc* changes are then made to reflect the unusual effects on turbulence of swirl, curved streamlines or rotation of the coordinate system. Typically one makes the lengthscale depend on Richardson number or adds terms to the dissipation equation and calibrates to match observed behaviour. This approach does not make use of the mathematical requirements that the dependent variables and their evolution equations must satisfy and leads to models that perform poorly when used in situations substantially different from the benchmark flows for which they have been calibrated. There is no reason why

a second-order modelling method cannot be successfully applied to a high-Reynolds-number rotating turbulence: no new unknown terms appear in the equations and, for moderate Rossby number, very little of the phenomenology on which the method is based changes.

The effect of rotation on the second-order moments is felt through the rapid-pressure–velocity correlation and the Coriolis terms. The difficulty with the equations, as modelled up to now, can be seen when the equations are transformed to a rotating coordinate system: they are not materially frame indifferent in the two-dimensional limit. This requirement, expressed in the context of a Taylor–Proudman reorganization, $\Omega_j u_{i,j} = 0$, has been named the principle of two-dimensional frame invariance (2DMFI) by Speziale (1989). There are, in fact, a number of flow fields that are materially frame indifferent (MFI) and 2DMFI is a subset of a larger class of such flows (as will be described more precisely).

The problem with the current modelled second-order equations results from the inability of the rapid-pressure correlation model to reflect the physics associated with the reduction of stretching of vorticity in a particular direction. Such phenomena, occurring in a variety of flows, are most readily seen in the context of Taylor–Proudman effects occurring in bounded rotating flows. As the flow becomes two-dimensional, in the limit of rapid rotation (about a vertical coordinate), the flow becomes horizontally divergence free and the evolution equations become independent of the rotation of the frame. This is a form of realizability: in a particular class of flows that are horizontally non-divergent the turbulence is MFI and so should the set of modelled equations be. Mathematically this requires the rapid-pressure covariance representation, appearing on the right-hand side of the second-order moment equations, to equal the Coriolis terms, in order to make the equations frame invariant. A rapid-pressure model consistent with these facts – reflecting more of the information contained in the Navier–Stokes equations – is required if one is to compute more complex three-dimensional flows.

As a general tool is being developed to compute a wide class of flows, for which there may not be well-documented benchmark flows with which to calibrate coefficients, it is necessary to construct a model from first principles incorporating more of the physics. In the present representation for the rapid-pressure–strain correlation the use of calibration constants, which do not come from first principles, have been minimized. This is done this by requiring the representation to have the proper behaviour in five different limits. The representation must be: (i) frame invariant for a number of, not unusual, flow situations that are horizontally divergence free; (ii) realizable when an arbitrary eigenvalue of the Reynolds stress vanishes; (iii) jointly realizable when an eigenvalue of the tensor $\langle\theta\theta\rangle\langle u_i u_j\rangle - \langle\theta u_i\rangle\langle\theta u_j\rangle$ vanishes; (iv) satisfy the isotropic limit; and (v) be asymptotically consistent with a stationary state of the turbulence, $(\mathrm{D}/\mathrm{D}t)\, b_{ij} = 0$. Of these five principles the last one is a statement based on experimental approximation rather than mathematical fact. It is tacitly assumed that for a specific class of flows, to a reasonable approximation, there exists an equilibrium state to which the flow relaxes upon the removal of any perturbing forces.

Ensuring the proper frame invariance of the modelled second-moment equations is done by requiring that the rapid-pressure–velocity correlation representations in the heat-flux and Reynolds stress equations satisfy the 'geostrophic' constraints (Ristorcelli 1987; Ristorcelli & Lumley 1991*b*):

$$\epsilon_{pqn}\Omega_n X_{ipqj} = \epsilon_{qjn}\Omega_n\langle u_i u_q\rangle, \tag{1}$$

$$\epsilon_{pqn}\Omega_n X_{pqi} = \epsilon_{qin}\Omega_n\langle u_q\theta\rangle, \tag{2}$$

where X_{ipqj} and X_{pqi} are the volume integrals of the two-point covariance that make up the rapid-pressure covariance. The meaning of these constraints will be made clear during the course of their derivation. Some preliminary discussion is given here to provide a context for subsequent developments.

The term geostrophic is borrowed from the meteorological literature where it is used to describe the low-Rossby-number balance between Coriolis and pressure forces in the evolution equations of the large-scale atmosphere (Lesieur 1991). A very simple and elegant physical demonstration of the two-dimensionalization of the large scales of a flow by rotation is given in the rotating tank experiments of Hopfinger, Browand & Gagne (1982). The constraint, however, is independent of how the flow is two-dimensionalized and is, therefore, independent of Rossby number. Taylor–Proudman-type flows are actually a subset of a class of flows that are frame indifferent. The set consists of flows in which (i) $u_3 = 0$, or (ii) the velocity is independent of the coordinate along the axis of rotation, or (iii) the vertical velocity equation is in hydrostatic balance. All of these flows are horizontally divergence free and are therefore characterized by an absence of vortex stretching along the axis of rotation. The condition of being horizontally divergence free is necessary for MFI.

The present article is a description, derivation and validation of a representation for the rapid-pressure covariance that ensures the frame invariance of the modelled Reynolds stress when the large scales of the motion become horizontally non-divergent. This representation also satisfies the principle of two-dimensional material frame indifference. It is not, however, the first rapid-pressure model to have satisfied this principle; the constant coefficient model of Haworth & Pope (1986) is also frame indifferent in the two-dimensional limit. Part of the present derivation has been given earlier in departmental reports (Ristorcelli 1987, 1991; Ristorcelli & Lumley 1991*b*), but in those previous developments of the model several free parameters were, for simplicity, set to zero. In this extension of that work the stationary points of the homogeneous shear are used to set free parameters occurring in the model. This ensures that the fixed points of the modelled differential equations are the same as the experimentally observed fixed points of a particular physical flow. This is done without sacrificing any of the mathematical principles built into the model.

The next section of this article defines and specifies the problem. Section 3 presents a derivation of the tensor polynomial model for the rapid-pressure correlation; the constraints and a derivation of the new geostrophic constraint are presented and discussed (§4). Also included (§5) is a mathematically precise definition of the types of fields that lead to frame indifferent evolution equations. It will be seen that there are several flow situations for which material frame indifference is an important consideration especially if a general model is sought. A new ansatz for the rapid-pressure correlation produces a model valid away from both the geostrophic – or horizontally divergence free – and realizability limits (§6). Section 7 uses results from matrix algebra to collapse the model to a structure similar to other rapid-pressure models with some interesting differences. The model is seen to have the same tensor bases as the FLT model (Fu, Launder & Tselepidakis 1987) and in the limit of a planar mean flow it has the same tensor bases as the quasi-linear SSG model of Speziale, Sarkar & Gatski (1991). Sections 8 and 9 show computations done with the model and compare the results to other models. Following this in §10 a general discussion of various modelling issues such as realizability, the limitation of constant coefficient models and the use of fixed points as a limit for calibrating turbulence models is given.

2. The rapid-pressure covariance

In incompressible turbulence in a rotating coordinate system, with buoyancy effects in the Boussinesq approximation, the Reynolds stress equations have the following form:

$$\frac{\mathrm{D}}{\mathrm{D}t}\langle u_i u_j\rangle + 2(\epsilon_{ikp}\langle u_p u_j\rangle + \epsilon_{jkp}\langle u_p u_i\rangle)\,\Omega_k\, Ro^{-1}$$
$$= \langle\theta u_i\rangle\beta_j + \langle\theta u_j\rangle\beta_i - [\langle u_j u_p\rangle U_{i,p} + \langle u_i u_p\rangle U_{j,p}] - \langle u_i u_j u_p\rangle_{,p}$$
$$- [\langle p_{,j} u_i\rangle + \langle p_{,i} u_j\rangle] + Re^{-1}\langle u_i u_j\rangle_{,pp} - 2Re^{-1}\langle u_{i,p} u_{j,p}\rangle, \tag{3}$$

$$\frac{\mathrm{D}}{\mathrm{D}t}\langle\theta u_i\rangle + 2\epsilon_{pik}\,\Omega_k\langle\theta u_p\rangle\, Ro^{-1} = -[\langle\theta u_j\rangle U_{i,j} + \langle u_i u_j\rangle T_{,j}] + \langle\theta\theta\rangle\beta_i$$
$$- \langle\theta u_i u_j\rangle_{,j} - \langle p_{,i}\theta\rangle + Re^{-1}(1+Pr^{-1})(\langle\theta u_i\rangle_{,jj} - 2\langle\theta_{,j} u_{i,j}\rangle. \tag{4}$$

The velocity has been normalized by a characteristic velocity u_c and the Rossby number is $Ro = u_c/\Omega R_c$ where R_c is a lengthscale and Ω the rotation rate of the frame of reference. The gravity and rotation vectors are aligned with the 3-axis. Our concern is with the pressure–velocity and –temperature correlations, $\langle p_{,j} u_i\rangle$ and $\langle p_{,i}\theta\rangle$. An equation for the pressure fluctuations comes from the divergence of the Navier–Stokes equations for the fluctuating velocity:

$$u_{i,t} + u_j U_{i,j} + U_j u_{i,j} + + u_j u_{i,j} - \langle u_i u_j\rangle_{,j} + 2\epsilon_{ikp}\,\Omega_k u_p\, Ro^{-1} = -p_{,i} + \theta\beta_i + Re^{-1}u_{i,jj}, \tag{5}$$

which produces a Poisson equation for fluctuating pressure. The standard linear decomposition recognizes three terms:

$$-p^r_{,ii} = 2[U_{i,p} + \epsilon_{pik}\,\Omega_k\, Ro^{-1}]\,u_{p,i}, \tag{6}$$
$$-p^s_{,ii} = u_{i,j} u_{j,i} - \langle u_{i,j} u_{j,i}\rangle, \tag{7}$$
$$p^b_{,ii} = \beta_i\theta_{,i}, \tag{8}$$

where p^r, p^s, p^b are respectively the rapid pressure, the slow or return-to-isotropy pressure, and the buoyancy pressure. The effects of rotation are felt through the rapid pressure, p^r. Solution of the Poisson equation for the rapid pressure is by application of Green's theorem:

$$\phi(\boldsymbol{x}) = -(4\pi)^{-1}\int\phi(\boldsymbol{x}')_{,jj}\,\mathrm{d}\boldsymbol{x}'/(\boldsymbol{x}-\boldsymbol{x}').$$

It is the moments of the solution that are required to close the second-order equations. For a homogeneous mean field, more than an integral scale away from any surfaces, a straightforward interchange of the order integration and averaging produces:

$$\langle p^r{}_{,j} u_i\rangle + \langle p^r{}_{,i} u_j\rangle = -2[U_{q,p} + \epsilon_{pqk}\,\Omega_k\, Ro^{-1}][X_{ipqj} + X_{jpqi}], \tag{9}$$
$$\langle p^r{}_{,i}\theta\rangle = -2[U_{q,p} + \epsilon_{pqk}\,\Omega_k\, Ro^{-1}]\,X_{piq}, \tag{10}$$

where

$$X_{piq} = (4\pi)^{-1}\int\langle\theta(\boldsymbol{x})\,u_p(\boldsymbol{x}')\rangle_{,i'q'}\,\mathrm{d}\boldsymbol{x}'/(\boldsymbol{x}-\boldsymbol{x}'), \tag{11}$$

$$X_{ipqj} = (4\pi)^{-1}\int\langle u_i(\boldsymbol{x})\,u_p(\boldsymbol{x}')\rangle_{,j'q'}\,\mathrm{d}\boldsymbol{x}'/(\boldsymbol{x}-\boldsymbol{x}'). \tag{12}$$

The construction of a tensor polynomial model for the volume integrals of the two-point correlations, X_{ijkl} and X_{ijk}, is the subject of this article. The rapid-pressure covariance integral appearing in the heat-flux equations, X_{ijk}, is treated as the Reynolds stresses and the heat fluxes are linked through Cauchy–Schwarz inequalities,

$\langle\theta\theta\rangle\langle u_i u_j\rangle - \langle\theta u_i\rangle\langle\theta u_j\rangle \geqslant 0$ and their modelling cannot be done independently. The rapid-pressure term appearing in the Reynolds stress equations necessary to treat the mechanical turbulence problem is the focus of this article.

3. A representation for the rapid-pressure covariance

A constitutive relation in which the integral of the two-point covariance is parameterized by a local function of the anisotropy tensor and heat-flux vector is proposed. The most general forms of such relationships are the following tensor polynomials:

$$\begin{aligned}
X_{ijkl}/\langle u_p u_p\rangle = {} & A_1\delta_{ij}\delta_{kl} + A_2(\delta_{ik}\delta_{jl} + \delta_{il}\delta_{jk}) \\
& + A_3\delta_{ij}b_{kl} + A_4 b_{ij}\delta_{kl} + A_5(b_{ik}\delta_{jl} + b_{il}\delta_{jk} + \delta_{ik}b_{jl} + \delta_{il}b_{jk}) \\
& + A_6\delta_{ij}b_{kl}^2 + A_7 b_{ij}^2\delta_{kl} + A_8(b_{ik}^2\delta_{jl} + b_{il}^2\delta_{jk} + \delta_{ik}b_{jl}^2 + \delta_{il}b_{jk}^2) \\
& + A_9 b_{ij}b_{kl} + A_{10}(b_{ik}b_{jl} + b_{il}b_{jk}) \\
& + A_{11}b_{ij}b_{kl}^2 + A_{12}b_{ij}^2 b_{kl} + A_{13}(b_{ik}^2 b_{jl} + b_{il}^2 b_{jk} + b_{ik}b_{jl}^2 + b_{il}b_{jk}^2) \\
& + A_{14}b_{ij}^2 b_{kl}^2 + A_{15}(b_{ik}^2 b_{jl}^2 + b_{il}^2 b_{jk}^2),
\end{aligned}$$

$$\begin{aligned}
X_{pkj} = {} & D_1\langle\theta u_p\rangle\delta_{kj} + D_2(\langle\theta u_k\rangle\delta_{pj} + \langle\theta u_j\rangle\delta_{pk}) \\
& + D_3\langle\theta u_p\rangle b_{kj} + D_4(\langle\theta u_k\rangle b_{pj} + \langle\theta u_j\rangle b_{pk}) \\
& + D_5\langle\theta u_p\rangle b_{kj}^2 + D_6(\langle\theta u_k\rangle b_{pj}^2 + \langle\theta u_j\rangle b_{pk}^2) \\
& + [D_7 b_{qp}\delta_{kj} + D_8(b_{qk}\delta_{pj} + b_{qj}\delta_{pk})]\langle\theta u_q\rangle \\
& + [D_9 b_{qp}b_{kj} + D_{10}(b_{qk}b_{pj} + b_{qj}b_{pk})]\langle\theta u_q\rangle \\
& + [D_{11}b_{qp}b_{kj}^2 + D_{12}(b_{qk}b_{pj}^2 + b_{qj}b_{pk}^2)]\langle\theta u_q\rangle \\
& + [D_{13}b_{qp}^2\delta_{kj} + D_{14}(b_{qk}^2\delta_{pj} + b_{qj}^2\delta_{pk})]\langle\theta u_q\rangle \\
& + [D_{15}b_{qp}^2 b_{kj} + D_{16}(b_{qk}^2 b_{pj} + b_{qj}^2 b_{pk})]\langle\theta u_q\rangle \\
& + [D_{17}b_{qp}^2 b_{kj}^2 + D_{18}(b_{qk}^2 b_{pj}^2 + b_{qj}^2 b_{pk}^2)]\langle\theta u_q\rangle,
\end{aligned}$$

where b_{ij} is the anisotropy tensor $b_{ij} = \langle u_i u_j\rangle/\langle u_q u_q\rangle - 1/3\delta_{ij}$ and $\langle\theta u_i\rangle$ is the turbulent heat flux. Following Pope's linearity principle only terms linear in the heat flux are kept. The A_i and D_i are functions of the invariants of b_{ij} and $\langle\theta u_i\rangle$.

As complex as these expressions appear one should keep in mind that they result from nothing more complex, in concept, than a Buckingham *PI* theorem. For tensor quantities invariance under a larger group of transformations is required. The objective is to ensure that the above parameterization has as many of the mathematical properties as the original quantity, X.

Parameterizing the integral of a two-point correlation in terms of the local anisotropy tensor based on the Reynolds stress is a substantial simplification requiring consideration. For turbulence with a short term memory and limited awareness Lumley (1970) has discussed the conditions under which such a constitutive relation is tenable. Lumley (1967) carried out an expansion procedure to indicate how the truncation errors scale. From one point of view, the constitutive relation proposed can be seen as the first term in a functional Taylor series expansion for the rapid-pressure correlation. As the correlation decays with distance the primary contribution to the integral will come from regions within an integral lengthscale of the local position. In a quasi-homogeneous turbulence, homogeneous over a scale ℓ, the first term will constitute a good approximation. Retaining higher-order terms of the functional Taylor series expansion which involves spatial and temporal derivatives of b_{ij}

substantially complicates the problem. It is expected that the retention of only the first-order term captures enough of the physics to allow prediction suitable for engineering purposes.

The parameterization above is not expected to be valid for $Ro \ll 1$ or in other situations when the two-point statistics are strongly anisotropic and not characterizable by a single integral scale. Consider that the two-point velocity covariance appearing in the integrand is related to the spectral energy density tensor; thus the proper parameterization of the rapid pressure is equivalent to the proper parameterization of the spectral energy density tensor. DNS indicates that rapidly rotating homogeneous turbulence with isotropic initial conditions will in general stay isotropic; that is when the anisotropy of the Reynolds stress is used as a measure of anisotropy. The fact is that the energy spectrum does not stay isotropic and the characterization of its anisotropy solely in terms of the Reynolds stresses in rapidly rotating turbulence is misleading. The coherence of the flow, in various directions, is substantially modified and substantially anisotropic and constitutive arguments put forward by Lumley (1967) assuming 'limited awareness' are no longer valid and must be reassessed. In such situations additional tensor quantities parameterizing the energy spectrum are necessary: perhaps the appropriate measure of the anisotropy of the energy spectrum is the anisotropy of the coherence. Perhaps the structural tensor ideas such as those put forward by Reynolds (1989) may be a step in the direction of handling flows in which such effects are important. The present theory is not one which is intended to cover the case of $Ro \ll 1$ for which such a simple parameterization of the energy spectrum is impossible.

In the light of the unusual effects of rotation the usefulness of other assumptions made in these types of closures also requires investigation. In addition to comments made in invoking the above constitutive relation there are several phenomena, peculiar to rotating flows, that may be in conflict with assumptions made in such single-point closures which will limit the modelling to a specific class of flows. In particular the inertial wave field associated with the rotation may interfere with: (i) the energy cascade from the large to the small scales of the flow, (ii) the universal equilibrium assumed for the small scales of the flow, and (iii) the assumed steadiness of the mean flow as it effects the assumption of stationarity of the turbulence statistics. The first two of these issues deals with the parameterization of the spectral cascade and is therefore an issue involving the dissipation equation. These issues are now individually considered.

In a time-varying mean flow rotating with speed Ω there will be low-frequency inertial oscillation: frequencies primarily lower than but up to 2Ω. For a quasi-steady assumption to be valid, changes in the mean flow must be slow with respect to the turbulence's ability to adjust to the imposed changes in the mean. This requires that $2\Omega < \epsilon/k$ and becomes a lower bound for a Rossby number, $Ro = \epsilon/2\Omega k > 1$, for which a quasi-equilibrium theory is appropriate.

Similar to a stably stratified density field in which stratification inhibits particle motions in the vertical direction, rotation inhibits transverse displacements of fluid particles. Similar to the radius of gyration of a charged particle in a magnetic field, the lateral displacement of a turbulent fluid element in a rotating frame can be characterized by a lengthscale $(q^2/3)^{1/2}/2\Omega$ where $q^2 = \langle u_j u_j \rangle$. This lengthscale must be larger than the turbulence lengthscale $\ell \sim (q^2/3)^{3/2}/\epsilon$ to ensure that the transverse confinement by the Coriolis forces does not affect the motions associated with the cascade of the fluctuating field. This produces a similar bound on the turbulent Rossby number $Ro = \epsilon/2\Omega k > 3/2$.

The phase coherence necessary for the cascade of energy to the smaller scales of the motion will be interfered with if the production scales of the motion $\kappa\ell \sim 1$, where κ is the wavenumber, are subject to an inertial wave field. The inertial wave interference with the nonlinear cascade mechanism will make the current parameterizations for the dissipation invalid. There are some limits on the rotation rate that can be set in order for the current parameterization of the cascade to be adequate. Consider the Rossby number defined as a ratio of the vorticity of the production scales of the motion to the background vorticity $Ro_t = (q^2/3)^{1/2}/2\Omega\ell = 3\epsilon/2\Omega q^2$ using $\epsilon = (q^2/3)^{1/2}/\ell$. A spectral Rossby number can also be defined as $Ro(\kappa) = u(\kappa)/2\Omega\ell(\kappa) = (\kappa E(\kappa))^{1/2}/2\Omega(2\pi/\kappa)$ which using the inertial range scaling $E(\kappa) = \alpha\epsilon^{2/3}\kappa^{-5/3}$ and $\epsilon = (q^2/3)^{1/2}/\ell$ becomes $Ro(\kappa) \sim 0.2\ (\kappa\ell)^{2/3} Ro_t$. The effects of rotation decrease as the wavenumber increases. For the inertial oscillations associated with the rotation not to interfere with the cascade mechanism $Ro(\kappa) > 1$ for $\kappa\ell \sim 2$ is required. Thus for $Ro_t > 3$ the usual parameterization of the spectral cascade rate, ϵ, in terms of the energy-containing scales of the motion is appropriate. For $Ro_t < 3$ the current dissipation equation begins to require modification. How the dissipation equation is to be changed to account for the effects of rotation on the cascade rate is an unresolved issue that is the topic of current research. It is, however, clear that the assumption of the small-scale equilibrium with the large scales of the motion is valid in most high-Reynolds-number rotating flows of interest if $Ro_t > 1$: the Rossby number of the dissipation scales of the motion is $Ro_\epsilon = Re_\ell^{1/2}\, Ro_t$ and therefore the dynamics of the small-scale motions are not directly dependent on the effects of rotation for $Ro_t > 1$.

Thus the Rossby number of the dissipation scales of the flow is large and their dynamics are not influenced by the rotation and they can be assumed to be in equilibrium with larger scales of the flow (which are affected by rotation). This criterion is necessary to investigate to ensure the adequacy of the assumption of universal behaviour of the small scales. If this is not the case the smallest scales of the flow will have their own dynamics and will not be closely linked to the large scales of the flow through an inertial subrange characterized by a constant spectral flux and parameterizable by the large scales of the flow.

Having dealt with some phenomenological issues and their implications on bounds for the Rossby number for which a representation of the rapid pressure is being sought, the mathematical nature of the rapid-pressure–velocity and –temperature covariances are now investigated.

4. The geostrophic constraint

The geostrophic constraint is now derived and discussed. The issue of material frame indifference is discussed first: it is the physical fact that leads to the geostrophic constraint. There are a variety of flows that are materially frame indifferent (MFI). For turbulence in which the velocity field does not depend on the coordinate along the axis of rotation Speziale (1985, 1989) has shown that the incompressible Navier–Stokes equations are MFI. It will be seen that *materially frame indifferent fields are horizontally divergence-free velocity fields*, $u_{,x} + v_{,y} = -w_{,z} = 0$. MFI is, in fact, related to the absence of the stretching of vorticity along the axis of rotation and not necessarily the coordinate independence of the flow. MFI fields include velocity fields which have no component along the axis of rotation, as is seen in Taylor–Proudman-type flows in bounded domains. They also includes flows with strong stable stratification or in small aspect ratio situations. These ideas are made more precise in the following developments.

First, a point on nomenclature: Reynolds' (1989) nomenclature will be adopted for these discussions. A velocity field that is a function of two dependent variables will be called two-dimensional. A velocity field in which the velocity vector has only two components but, in general, can depend on three dependent variables will be called two-componential.

A horizontally divergence-free velocity field can be represented in the following way:

$$u_p = \epsilon_{pqk}\Omega_k\psi_{,q} + \Omega_p u_i \delta_{i3} = \epsilon_{pqk}\Omega_k\psi_{,q} + \Omega_p w; \tag{13}$$

incompressibility leads to the horizontally divergence-free condition,

$$u_{p,p} = \Omega_p u_{i,p}\delta_{i3} = \Omega_3 w_{,z} = 0. \tag{14}$$

For general $\psi = \psi(x, y, z)$ inversion produces

$$\psi_{,p} = \epsilon_{qpk}\Omega_k u_q + \Omega_p\Omega_q\psi_{,q}. \tag{15}$$

Note that this representation includes as some special cases: (i) two-component velocity fields whose velocity components lie in planes perpendicular to the axis of rotation, $\Omega_j u_j = 0$, or (ii) three-component velocity fields that are independent of the dependent variable along the axis of rotation, $\Omega_j u_{i,j} = 0$, for which $\psi = \psi(x, y)$ and

$$\psi_{,p} = \epsilon_{qpk}\Omega_k u_q. \tag{16}$$

For a streamfunction $\psi = \psi(x, y, z)$, the vorticity is

$$\omega_i = \Omega_l\psi_{,il} - \Omega_i\psi_{,qq}. \tag{17}$$

The vertical component of the vorticity is given by the horizontal Laplacian of the streamfunction:

$$\omega_3 = -\nabla_H^2\psi, \tag{18}$$

which evolves according to the vertical component of the curl of the Navier–Stokes equations:

$$\dot{\omega}_3 + u_j\omega_{3,j} = (\omega_j + 2\Omega_j)u_{3,j} + \nu\omega_{3,jj}. \tag{19}$$

This is the prognostic equation for the streamfunction and for several flows it is closed with respect to the streamfunction: all the quantities in the equation are known as a function of $\psi(x, y, z)$. The velocities appearing as coefficients are functions of the streamfunction or, in the case of u_3, obey a linear passive-scalar-type equation independent of rotation for a particular class of flows. Inspection shows that the vertical vorticity equation is frame invariant if there is no stretching of vorticity along the axis of rotation; that is when the flow is horizontally divergence free, $\Omega_j u_{3,j} = 0$. (The boundary conditions are assumed to be independent of rotation.) As u_1 and u_2 are determined by the streamfunction, it merely remains to see under what conditions the evolution of u_3 is also frame invariant. The classes of flows for which this type of reasoning is appropriate are now investigated in more depth.

The simplest MFI flow is one in which $w = 0$. The whole flow evolves according to one equation, that for the vertical vorticity. In the absence of w there is no axial stretching of vorticity and the vertical vorticity equation is MFI. Let it be described in the following way.

Case 1. $\Omega_j u_j = 0$, $\psi = \psi(x, y, z)$

Using Reynolds' nomenclature this flow can be called *two-componential* (2C); it is not, however, two-dimensional. The streamfunction can be a function of all three coordinate directions and the field is horizontally divergence free as there is no velocity

along the axis of rotation. Lack of horizontal divergence, which is achieved because $w = 0$, is a sufficient condition for MFI of this flow. This might correspond to the flow after turbulent collapse in a stably stratified medium. Lesieur (1991) or Métais & Herring (1989) have discussed and investigated such phenomena. A noteworthy aspect of such flows is the strong vertical variability leading to a vertical shear thought to be responsible for a major portion of the dissipation.

In addition to covering strongly stratified flows and large Brunt–Väisällä frequency, case 1 also covers flows in low-aspect-ratio situations, $H/L \to 0$. Investigation of the non-dimensional continuity equation shows $w \to 0$ as $H/L \to 0$. Such a flow also includes mesoscale and global geophysical flows.

A different class of flows is now addressed, which are of interest in geophysical applications and require the Rossby number be small. The Navier–Stokes equations in a rotating frame, in the Boussinesq approximation, and in dimensional form, are

$$u_{i,t} + u_j u_{i,j} + 2\epsilon_{ikp}\Omega'_k u_p = -(1/\rho)p_{,i} + \beta g\theta\delta_{3i} + \nu u_{i,jj}. \tag{20}$$

Non-dimensionalizing the equation with respect to the characteristic vertical and horizontal velocities (W_c, U_c) and dimensions (H, L), the highest-order terms, to order Rossby number, in the horizontal momentum equations are

$$u_{i,t} + 2\epsilon_{ikp}\Omega'_k u_p = -(1/\rho)p_{,i}. \tag{21}$$

The time-derivative term is order $(\Omega T)^{-1}$ with respect to the Coriolis and pressure balance. For scales of the motion in which $\Omega T \gg 1$ the geostrophic balance ensues:

$$2\epsilon_{ikp}\Omega'_k u_p = -(1/\rho)p_{,i}; \tag{22}$$

the streamfunction and the pressure are identical quantities (*modulo* constants of proportionality) as can be verified by substitution of the representation of the velocity in terms of the streamfunction into the geostrophic balance. The equation for the vertical velocity is

$$w_{,t} + u_j w_{,j} = -(1/\rho)p_{,z} + \beta g\theta + \nu w_{,jj}. \tag{23}$$

In the absence of buoyancy this equation is MFI if the flow is horizontally divergence free since the ψ-equation is MFI when horizontally divergence free $\Omega_j u_{3,j} = 0$. Note that the pressure and velocity in the w-equation are generated by ψ. This appears to be regardless of the dimensionality of the flow, i.e. for all $\psi = \psi(x, y, z)$, until the geostrophic balance of the horizontal vorticity equation is investigated:

$$2\Omega'_k u_{p,k} = 0. \tag{24}$$

Consistency requires that the flow depend only on the velocity coordinates in planes perpendicular to the axis of rotation – the flow is two-dimensional in the sense of $\psi = \psi(x, y)$. Let it be called the geostrophic balance in the absence of buoyancy and denote it case 2.

In the cases described above, a streamfunction is suggested by either kinematic issues, $H/L \to 0$, or by a balance of the dynamical equations, $Ro \to 0$. The arguments are asymptotic and suggest physical situations in which MFI is a consideration. The fact is, any three componential, two-dimensional flow, $w = w(x, y)$ and $\psi = \psi(x, y)$, is MFI. This is the case that Reynolds' (1994) treats and is the flow on which Speziale (1985) based his 2DMFI principle. In this case a streamfunction is postulated and one investigates under what conditions it leads to a MFI flow. Reynolds (1994) proof is a little different from that of Speziale (1989). Reynolds proves MFI by showing that the Coriolis terms in the momentum equations can be absorbed into the pressure, leaving the three momentum equations independent of the rotation if and only if $\psi = \psi(x, y)$.

MFI can easily be shown by noting that such a field is horizontally divergence free and thus the vertical vorticity equation is frame invariant and, because of the independence of the flow on z, the w-equations satisfy a MFI passive scalar equation. This case and the geostrophic flow are covered in case 2.

Case 2. $\Omega_j u_{i,j} = 0$, $\psi = \psi(x, y)$

Such a field is horizontally divergence free, which is a necessary but not sufficient condition, as indicated by the constraints placed on the coordinate dependence of the flow field by the horizontal vorticity equation. Note that the velocity field can still have three components and that its vertical component obeys a passive scalar equation. The Taylor–Proudman theorem is consistent with such a flow field. Note that in very common flows, a bounded domain with no-flux boundary conditions such that $\Omega_p u_p = 0$ on the boundary, the $\Omega_j u_{i,j} = 0$ case includes $\Omega_j u_j = 0$. The Taylor–Proudman theorem applied in an unbounded domain is included in this category.

A similar result is possible when buoyancy enters the geostrophic balance. The geostrophic balance of the horizontal components of the vorticity equation produce the following diagnostic relationship:

$$-2\Omega'_k u_{p,k} = \beta g \theta_{,k} \epsilon_{pk3}. \tag{25}$$

Consistency requires the temperature to be directly related to the streamfunction; the pressure and temperature are related according to a hydrostatic balance. This class of flows is delineated mathematically in the following way.

Case 3. $\Omega_j u_{i,j} \delta_{i3} = 0$, $\psi = \psi(x, y, z)$

The streamfunction is a function of all three coordinate directions though now $w = w(x, y)$. Thus for this class of flows or for the scales of the motion where $\Omega T \gg 1$, lack of horizontal divergence is a sufficient condition for MFI.

Note that these results require low Rossby number but do not require a small aspect ratio. In the small-aspect-ratio case, $H/L \to 0$, and lack of horizontal divergence and $w \to 0$ are asymptotically equivalent statements both leading to MFI flows as already indicated. A situation similar to the low-aspect-ratio or strongly stratified cases occurs when magnetic forces act to suppress the vertical component of the velocity field.

To summarize the perorations above, it has been shown that when the flow is horizontally divergence free the vertical vorticity equation, which is the evolution equation for the streamfunction, is MFI. MFI of the whole field is then determined by the nature of the equation for the vertical velocity. If (i) $w = 0$, or (ii) the pressure is independent of the axial coordinate or (iii) determined by a hydrostatic balance with the temperature, then the flow will be MFI. There may be other situations.

For the modelled set of second-order equations to be MFI in the specific flow conditions mentioned, the rapid-pressure correlations must satisfy the 'geostrophic' constraints,

$$\epsilon_{pqn} \Omega_n X_{ipqj} = \epsilon_{qjn} \Omega_n \langle u_i u_q \rangle, \tag{26}$$

$$\epsilon_{pqn} \Omega_n X_{pqi} = \epsilon_{qin} \Omega_n \langle u_q \theta \rangle. \tag{27}$$

A proof of this constraint is now given for $\psi = \psi(x, y)$. Consider the portion of the rapid-pressure correlation associated with the rotation:

$$\epsilon_{pqk} \Omega_k Ro^{-1} X_{ipqj} = \frac{1}{4\pi Ro} \int \epsilon_{pqk} \Omega_k \langle u_i(\boldsymbol{x}) u_p(\boldsymbol{x}') \rangle_{,j'q'} \frac{\mathrm{d}\boldsymbol{x}'}{\boldsymbol{x} - \boldsymbol{x}'}. \tag{28}$$

Insert the expression for the velocity field in terms of the streamfunction into the

integral and contract to produce, in the integrand, the Laplacian of the streamfunction, $\psi_{,p} = \epsilon_{qpk}\Omega_k u_q$. This reduces the volume integral of a two-point statistic to a one-point statistic which is identical with the Coriolis terms,

$$\epsilon_{pqk}\Omega_k Ro^{-1} X_{ipqj} = Ro^{-1}\langle u_i \psi_{,j}\rangle = Ro^{-1}\epsilon_{pjk}\Omega_k \langle u_i u_p\rangle \tag{29}$$

after application of Green's theorem. The geostrophic constraint $\epsilon_{pqn}\Omega_n X_{ipqj} = \epsilon_{qjn}\Omega_n\langle u_i u_q\rangle$ then follows. Inserting this equality into the rapid-pressure covariance representation on the right-hand side of the Reynolds stress equations cancels the Coriolis terms appearing on the left-hand side of the equation, leaving the equations indifferent to rotation. A similar analysis produces the geostrophic constraint on the rapid-pressure covariance appearing in the heat-flux equation. The proof of the geostrophic constraint when $\psi = \psi(x, y, z)$ is more complex but easily enough obtained with some deep reflection using similar ideas.

Thus with the satisfaction of the geostrophic constraint the modelled second-order equations will be MFI when the flow field attains the non-trivial configurations given above. In the context of single-point closures in which the Reynolds stresses are used to model the correlation, there are some qualifications which will be made in the appropriate section below.

A point of clarification: geostrophic turbulence has small horizontal divergence because its spectral Rossby number is small for a sizeable portion of the scales of the motion. This latter qualification distinguishes it from a general flow with vanishing horizontal divergence (that is made so by some other means) for arbitrary Rossby number. Both, however, are frame indifferent, and, depending on boundary conditions, both can also have a velocity field with only two vector components.

In most flows of engineering interest the flow field is bounded and has no-flux (or only mean-flux) boundary conditions. In such situations the MFI flow field will have a velocity field with two components, in the sense of $\Omega_j u_j \to 0$ or its statistical equivalent, $\Omega_j\langle u_j u_p\rangle \to 0$. Note carefully that this does not mean, in general, that $\Omega_k\langle u_j u_{p,k}\rangle \to 0$ as it would if the velocity field were independent of the axial coordinate. It is this vision of a 'typical' flow of engineering interest that underlies this article and that will play a role in the choice of an ansatz. It should be clear that an MFI field can, in general, have three non-zero vector components and be dependent on three coordinate directions. However, an engineering tool is being designed, and in the class of boundary conditions which are typical of engineering flows in bounded domains, MFI flow is typically accompanied by a vanishing $\Omega_j u_j$. It is for this specialization that the representation for the rapid-pressure covariance is constructed; it might well be called a '2CMFI' representation, in the sense that vanishing of $\Omega_j u_j$ leads to the MFI condition. The model has been called, in an earlier incarnation, a '2DMFI' model, in acknowledgement of the 2DMFI principle put forward by Speziale (1981, 1985, 1989), that suggested this work.

It should be kept in mind that the application of the MFI principles to obtain the geostrophic constraint is to be understood in an asymptotic sense. A turbulence model is not expected to compute flows that are MFI on all scales; this is a limitation inherent in single-point closures and the assumptions invoked to model the dissipation. Do reflect on the fact that the rapid-pressure strain is an integral over the energy spectrum of the turbulence: thus if only the first decade or so of scales of the motion are driven towards an MFI condition the rapid-pressure integral begins to behave as if that were the case.

5. Additional mathematical requirements

There are several statistical inequalities and mathematical identities that X must satisfy. These principles are used to obtain a set of algebraic constraint equations for the A_i and D_i. For arbitrary three-dimensional turbulence the tensor polynomials must satisfy the symmetry constraints

$$X_{ijkl} = X_{ijlk}, \quad X_{ijkl} = X_{jikl}, \quad X_{ijk} = X_{ikj}. \tag{30}$$

These symmetry constraints have already been built into the assumed form of the tensor polynomials. For arbitrary three-dimensional turbulence the tensor polynomials must also satisfy the constraints of normalization and continuity:

$$X_{ijkk} = \langle u_i u_j \rangle, \quad X_{ikk} = \langle u_i \theta \rangle, \quad X_{ijjk} = 0, \quad X_{iji} = 0. \tag{31}$$

Note that a contraction of the integral of a two-point statistic is a local one-point statistic. The tensors $\langle u_i u_j \rangle$ and $\langle \theta\theta \rangle \langle u_i u_j \rangle - \langle \theta u_i \rangle \langle \theta u_j \rangle$ are positive semi-definite. This reflects the fact that the energy of the turbulence is always positive and that the magnitude of the correlation coefficients between the various components of the tensors are bounded by one. These facts lead to the 'realizability' and 'joint-realizability' constraints which specify the behaviour of the correlations when specific limit states are approached. The relevant portion of the Reynolds stress transport equations, in principal axes, requires that

$$(\mathrm{D}/\mathrm{D}t)\langle u_\alpha u_\alpha \rangle \sim [U_{p,i} + \epsilon_{ipk}\Omega_k Ro^{-1}] X_{i\alpha p\alpha} \to 0 \quad \text{as} \quad \langle u_\alpha u_\alpha \rangle \to 0 \tag{32}$$

in order to satisfy realizability. The rate of change, due to the rapid-pressure correlation, of the eigenvalue $\langle u_\alpha u_\alpha \rangle$ is required to vanish as the limit state is approached. This ensures that the rapid-pressure correlation model does not cause the solution to go into the unrealizable region in which $\langle u_\alpha u_\alpha \rangle$ is negative. This realizability limit is rephrased in terms of the determinant of the Reynolds stress: $F = (R_{jj}^3 - 3R_{jj}R_{jj}^2 + 2R_{jj}^3)/6$ where $R_{ij} = \langle u_i u_j \rangle / \langle u_p u_p \rangle$ which can be written in terms of the invariants of the anisotropy tensor as $F = 1 + 9\mathrm{II} + 27\mathrm{III}$ where $\mathrm{II} = -\frac{1}{2}b_{ij}b_{ij} = -\frac{1}{2}\langle b^2 \rangle$, $\mathrm{III} = \frac{1}{3}b_{ip}b_{pj}b_{ji} = \frac{1}{3}\langle b^3 \rangle$. The determinant F varies between zero and one; $F = 1$ corresponds to an isotropic turbulence and $F = 0$ corresponds to the realizable limit in which one or more eigenvalues vanish.

Similar reasoning applied to the mixed tensor involving the Reynolds stress, the heat flux and the variance of the temperature fluctuations, produces the 'joint-realizability' constraint

$$(\mathrm{D}/\mathrm{D}t)D_{\alpha\alpha} \sim [U_{p,i} + \epsilon_{ipk}\Omega_k Ro^{-1}][\langle \theta\theta \rangle X_{i\alpha p\alpha} - \langle \theta u_\alpha \rangle X_{i\alpha p}] \to 0 \quad \text{as} \quad D_{\alpha\alpha} \to 0, \tag{33}$$

which couples the rapid-pressure correlations appearing in the heat-flux and the Reynolds stress equations. A similar determinant function F_d is defined with the normalized D_{ij}, for which $0 \leqslant F_d \leqslant 1$. Joint realizability reflects the requirement that the magnitude of the correlation coefficients be bounded by one: the Reynolds stress and the heat flux take on values 'jointly' such that the time rate of change of $D_{\alpha\alpha}$ vanishes as $D_{\alpha\alpha}$ goes to zero.

Note that no assumptions regarding the higher-order derivatives of the eigenvalue have been made. The strong form of realizability, in which $(\mathrm{D}^2/\mathrm{D}t^2)\langle u_\alpha u_\alpha \rangle > 0$ is required at the realizability limit in order to allow the turbulence to leave the realizable state, is not invoked. Such an agency is already present in the slow terms and it is not necessary to force the rapid terms to be responsible for such behaviour which, as will

be seen, is inconsistent with the small-parameter expansion of the rapid-pressure representation around the realizability limit. Instead a weak realizability constraint, as specified by Speziale, Abid & Durbin (1994) as a more general form of Pope's (1983) constraint, which does not allow the solution to attain the realizable limit in finite time, is invoked. This is done by requiring that the rapid-pressure correlation vanish more rapidly than the slow-pressure correlation model. This avoids any assumptions regarding the behaviour of the second derivative which are required for the flow to leave the realizable state which is accessible in finite time in models using the strong form of the realizability constraint. Moreover, recent work by Speziale *et al.* (1994) indicates that the present hierarchy of second-order models is inconsistent with the strong form of the realizability constraint. The rate of rotation of the eigenvalues arising from the second derivative is a sink term that cannot be balanced by the present models. In setting the portion of $(\mathrm{D}/\mathrm{D}t)\langle u_\alpha u_\alpha\rangle$ due to the rapid-pressure correlation to zero while choosing a return-term model that precludes accessibility of the realizable limit state, the weak form of realizability is satisfied by the sum of the modelled terms on the right-hand side of the transport equations. The issue raised by Speziale *et al.* (1994) does not impact on the present model, as all the higher-order derivatives vanish, and the realizable limit is not attainable in finite time because of the relative rate of disappearance of the slow-pressure terms with respect to the rapid-pressure terms. It may, however, require a rethinking of the modelling principles so that the intrinsic negativity of the second derivative can be properly balanced if the realizable limit is to be considered accessible.

It should also be kept in mind that the rapid-pressure covariance can be written as an integral of the energy spectrum over all the scales of the motion: from the production scales at $\kappa\ell \sim 1$, and larger, to the dissipation scales $\kappa\eta \sim 1$. The major contribution to the integral will be from the large scales of the motion. In turbulence with a $\kappa^{-5/3}$ inertial subrange in which there is enough of a separation of scales for a second-order simulation to be useful, say at least $Re_\ell \sim 10^4$, the ratio between the dissipative and the energy-containing lengthscales is $\eta/\ell \sim Re_\ell^{-3/4} \sim 1000$ and the flow scales range over $0 < \kappa\ell < 1000$. However, approximately 85% of the energy of the motion is contained in the first decade $\kappa\ell < 10$: the major contribution to the rapid-pressure integral is from the scales of the motion greater than one tenth of the production scales. If only the largest 1% of the flow scales, i.e. from $0 < \kappa\ell < 10$, begins to lose an eigenvalue of the Reynolds stress tensor, through some dynamical or kinematical agency, the rapid pressure will begin to approach the geostrophic (or for that matter the realizable) limit. The point is that, with any turbulence spectrum with a negative exponent, the rapid-pressure covariance can become asymptotically close to the frame-invariant limit with only a relatively small portion of the scales of the flow being horizontally divergence free.

6. Obtaining the variable coefficients in the representations

The application of the five sets of constraints – normalization, continuity, realizability, joint realizability and geostrophy – produces thirty-six linear algebraic equations (some of which are redundant) for the thirty-three unknown coefficients A_i, $(i = 1, 15)$ and D_i, $(i = 1, 18)$ appearing in the tensor polynomials. The equations are of the general form $A_{ij}(\mathrm{II}, \mathrm{III})\, x_j = b_i$ where $x_i = [A_1, \ldots, A_{15}, D_1, \ldots, D_{19}]$ and where II and III are the invariants of the anisotropy tensor, defined above. Using the definition $F = 1 + 9\mathrm{II} + 27\mathrm{III}$ the general form of the equations can be rewritten as $A_{ij}(\mathrm{II}, F)\, x_j = b_i$. Note that F and II appear linearly in the constraint equations.

The ansatz

$$X_{ijkl} = X^0_{ijkl} + FX^F_{ijkl}, \tag{34}$$

$$X_{ijk} = X^0_{ijk} + FX^F_{ijk} \tag{35}$$

is used to extract more information from the constraint equations. Here, $\boldsymbol{X}^0$ satisfies the set of constraint equations $A_{ij}(\mathrm{II}, 0)\, x^0_j = b_i$ obtained by application of all five sets of constraints which are simultaneously valid only when $F = 0$ (or equivalently when $\mathrm{III} = -(\mathrm{II} + \frac{1}{9})/3$), while the function $\boldsymbol{X}^F$ is obtained from a smaller set of equations $A_{ij}(\mathrm{II}, F)\, x^F_j = b^0_i$ which satisfy the three sets of constraints – normalization, continuity and joint-realizability – where b^0_i is a known function of the $\boldsymbol{X}^0$ solution. There are more unknowns than equations; the extra 'free parameters' will be used later to ensure that the model is asymptotically consistent with an equilibrium state. The solution, in which all free parameters are set to zero, and which satisfy all the mathematical constraints, will be called the basic model and has been given previously in Ristorcelli (1987, 1991) and Ristorcelli & Lumley (1991*b*).

The coefficients that satisfy all of the known mathematical requirements are:

$$A_1 = (111\mathrm{II} + 73)/27\mathrm{II}_d - F(420\mathrm{II} + 239)/135\mathrm{II}_d,$$

$$A_2 = -(69\mathrm{II} + 32)/27\mathrm{II}_d + F(420\mathrm{II} + 257)/270\mathrm{II}_d,$$

$$A_3 = (3\mathrm{II} + 4)/3\mathrm{II}_d - \tfrac{11}{10}F/(1 + 3\mathrm{II}),$$

$$A_4 = (15\mathrm{II} + 11)/3\mathrm{II}_d - \tfrac{4}{10}F/(1 + 3\mathrm{II}),$$

$$A_5 = -3(1 + 3\mathrm{II})/3\mathrm{II}_d + \tfrac{3}{10}F/(1 + 3\mathrm{II}), \quad A_6 = -(102\mathrm{II} + 61)/3\mathrm{II}_d,$$

$$A_7 = -2(33\mathrm{II} + 20)/3\mathrm{II}_d - \tfrac{6}{10}F/(1 + 3\mathrm{II}), \quad A_8 = (42\mathrm{II} + 23)/3\mathrm{II}_d,$$

$$A_9 = -(57\mathrm{II} + 28)/3\mathrm{II}_d - \tfrac{3}{10}F/(1 + 3\mathrm{II}),$$

$$A_{10} = (15\mathrm{II} + 14)/3\mathrm{II}_d + \tfrac{9}{10}F/(1 + 3\mathrm{II}),$$

$$A_{11} = -(102\mathrm{II} + 61)/\mathrm{II}_d, \quad A_{12} = -2(33\mathrm{II} + 20)/\mathrm{II}_d, \quad A_{13} = (42\mathrm{II} + 23)/\mathrm{II}_d,$$

$$A_{14} = 0, \quad A_{15} = 0,$$

where $\mathrm{II}_d = (1 + 3\mathrm{II})(7 + 12\mathrm{II})$, $F = 1 + 27\mathrm{III} + 9\mathrm{II}$, $\mathrm{II} = -\frac{1}{2}b_{ij}\, b_{ij}$ and $\mathrm{III} = \frac{1}{3}b_{ip}\, b_{pj}\, b_{ji}$. The rapid-pressure correlation integral, X_{pkj}, appearing in the heat-flux equations, is used to derive the A_i through the joint-realizability constraint. The general form of the third-order tensor polynomial used to model X_{pkj}, which cannot be obtained independent of the representation of X_{ijkl}, is included here for completeness:

$$D_1 = -(312\mathrm{II}^2 + 149\mathrm{II} - 21)/5\mathrm{II}_d - \tfrac{1}{5}F/(1 + 3\mathrm{II}),$$

$$D_2 = (48\mathrm{II}^2 + \mathrm{II} - 14)/5\mathrm{II}_d + \tfrac{3}{10}F/(1 + 3\mathrm{II}),$$

$$D_3 = -(324\mathrm{II}^2 + 222\mathrm{II} + 17)/\mathrm{II}_d - \tfrac{3}{10}F/(1 + 3\mathrm{II}),$$

$$D_4 = -3/(7 + 12\mathrm{II}) + \tfrac{9}{10}F/(1 + 3\mathrm{II}), \quad D_5 = -(102\mathrm{II} + 61)/\mathrm{II}_d,$$

$$D_6 = (42\mathrm{II} + 23)/\mathrm{II}_d, \quad D_7 = -2(3\mathrm{II} + 4)/5\mathrm{II}_d - \tfrac{3}{5}F/(1 + 3\mathrm{II}),$$

$$D_8 = 27(2\mathrm{II} + 1)/5\mathrm{II}_d, \quad D_9 = (42\mathrm{II} + 23)/\mathrm{II}_d, \quad D_{10} = (42\mathrm{II} + 23)/\mathrm{II}_d,$$

$$D_{13} = -8(39\mathrm{II} + 22)/5\mathrm{II}_d, \quad D_{14} = 2(24\mathrm{II} + 17)/5\mathrm{II}_d, \quad D_{15} = -27/(1 + 3\mathrm{II}).$$

Note that D_{11}, D_{12}, D_{16}, D_{17}, D_{18}, as well as A_{14}, A_{15} have been set to zero as they are not necessary to satisfy the constraints. The coefficients given above will be called the coefficients for the basic model, the portion of the model that satisfies all the known mathematical constraints, the eternal principles, if you will. To this basic model

additional terms, corresponding to the free parameters, are added in order to ensure that the model is asymptotically consistent with an experimentally observed equilibrium state of a particular turbulent flow field.

Some tacit assumptions and diverse subtleties are now amplified. The most important one relates to the assumed simultaneity of the materially frame indifferent state and the loss of an eigenvalue of the Reynolds stresses in the ansatz

$$X_{ijkl} = X^0_{ijkl} + FX^F_{ijkl}.$$

Note that $\boldsymbol{X}^0$ satisfies, simultaneously, both the geostrophic, $\Omega_j u_{i,j}\,\delta_{i3} = 0$ (more accurately $\Omega_j u_j\,\delta_{i3} = 0$), and realizability constraints, $(\mathrm{D}/\mathrm{D}t)\langle u_\alpha u_\alpha\rangle \to 0$ as $\langle u_\alpha u_\alpha\rangle \to 0$. This means that when $F \neq 0$, X does not satisfy the geostrophic constraints even though the flow could be MFI: which is to say that $\Omega_j u_j = 0$ is assumed to be the only way the modelled equation can become frame invariant. The frame-invariant condition, $\Omega_j u_{i,j}\,\delta_{i3} = 0$ was not used and it seems that such a constraint cannot be handled by this class of single-point closures. This limitation has been recognized by Reynolds (1994) and manifests itself as a directional singularity when the turbulence loses two eigenvalues, as discussed below. The limitation was recognized earlier when the tensorial representation for the rapid pressure was postulated: such a representation would not be valid for turbulence with a highly anisotropic two-point correlation. Thus, using the ansatz above, MFI cannot be satisfied unless $F = 0$, i.e. the eigenvalue of the Reynolds stress along the axis of rotation vanishes. The model is in fact a model that is only MFI in the two-component limit. This choice has been made with a typical engineering flow in mind and limits the model to flows in bounded domains with zero- or constant-(in time) flux boundary conditions. This is in acknowledgement of the fact that there is no statistically stationary flow with non-zero u_3 unless it is forced through the boundary conditions on u_3. The initial-condition problem is a decay problem since the energy exchange between $\langle u_3 u_3\rangle$ and the other components of the energy does not occur without the necessary pressure transfer term.

This suggests using the acronym '2CMFI' to describe this model, in recognition of the fact that the components of the fluctuating velocity field along the axis of rotation are asymptotically zero, and not because the flow is independent of that coordinate direction, which it may or may not be. The model has been called, in the past, a '2DMFI' model in acknowledgment of Speziales' constraint (1985, 1989).

The A_i are nonlinear functions of the invariants of b_{ij}: they are ratios of polynomials of the invariants. The realizability limit is attained along the line $\mathrm{III} = -(\mathrm{II} + \frac{1}{9})/3$ on which $F = 0$. At the isotropic limit $\mathrm{II} = \mathrm{III} = 0$ and $F = 1$, and thus $A_1 + A_2 = 1/10$ and the well-known exact result for isotropic turbulence is obtained. Note that the 'off-realizability' correction $F\boldsymbol{X}^F$ is necessary to obtain this limit. The satisfaction of the isotropic limit is discovered to be a consequence of the constraints used to create the 2DMFI model – it is not a constraint that has been enforced to obtain the model, but is satisfied naturally by the ansatz.

The choice of which free parameters to set to zero in the basic model is determined by the ordering in which the anisotropy of the flow is expressed. The crucial point is that it is possible to satisfy all the mathematical constraints with thirteen rather than fifteen coefficients for the mechanical rapid-pressure model. Other than that the choice is arbitrary; the physics is in the satisfaction of the constraints.

Note that the coefficients appear to be singular at the one-dimensional limit when $1 + 3\mathrm{II} = 0$. The singularity is not a $1/0$ singularity which results in computational difficulties; the singularities appearing in the individual terms in the rapid-pressure representation cancel each other when summed. The singularity is a directional

singularity as was discovered by Reynolds (1994). This stems from the fact that the parameterization of the energy spectrum in terms of the anisotropy tensor results in a rapid-pressure representation that cannot distinguish between turbulence with a vanishing eigenvalue and turbulence that is perfectly correlated in the direction of that eigenvalue (now no longer zero). This is to be expected when parameterizing the volume integral of a two-point statistic in terms of the local values of one-point statistics. It does not invalidate the method – it simply means that the method is not applicable to flows with strongly anisotropic coherences (or, equivalently, very large integral scales in a particular direction). The manifestation of this shortcoming is the fact that the expressions for the rapid-pressure covariance, when the flow loses two eigenvalues, depends on the relative rates at which the two eigenvalues are lost. This is a very interesting theoretical point and suggests the types of flows for which this class of models is unsuitable. From a practical viewpoint, for the class of flows for which such tensor polynomial representations are suitable the point is moot: one does not expect to compute a flow whose physics is inconsistent with the assumptions made to create the equations to represent the flow. A flow with strongly anisotropic coherences does not appear to be a flow for which the single-point closures, as they are presently understood, appears to be suitable.

It should be emphasized that the form of the rapid-pressure covariance was chosen so that the variable coefficients are valid for all states of the turbulence – they are not fixed to constant values which are only valid at some asymptotic state. It is this fact that distinguishes this representation from others at this time: the coefficients are functions of the state of the turbulence obtained by application of the mathematically known limit states. Furthermore, the limiting states of the turbulence are not used to set the coefficients or to calibrate the model: they are used to ensure that the variable coefficients are consistent with, not set by, the extreme states of the turbulence. The resulting model coefficients, therefore, satisfy all mathematical constraints for any arbitrary Reynolds stress – not just at the realizability or geostrophic limit states. The second term, FX^F, in the expression for X, represents the 'off-realizability correction'. Therefore, the coefficients, A_i and D_i, are functions dependent on the state of the turbulence as parameterized by the invariants and only attain their realizable limit values at $F = 0$.

7. A compact representation of the 2DMFI rapid-pressure model

The rapid-pressure correlation models are usually written in the form they appear in the Reynolds stress equations, with

$$\Pi_i^r = 2[U_{q,p} + \epsilon_{pqk}\Omega_k Ro^{-1}]X_{piq}, \tag{36}$$

$$\Pi_{ij}^r = 2[U_{q,p} + \epsilon_{pqk}\Omega_k Ro^{-1}][X_{ipqj} + X_{jpqi}], \tag{37}$$

which can be rewritten in terms of the strain and rotation tensors as

$$\Pi_{ij}^r = 2[S_{qp} + W_{qp}][X_{ipqj} + X_{jpqi}],$$

where $S_{qp} = \frac{1}{2}(U_{q,p} + U_{p,q})$ and $W_{qp} = \frac{1}{2}(U_{q,p} - U_{p,q}) + \epsilon_{pqk}\Omega_k Ro^{-1}$ are the usual mean strain rate and the total or intrinsic rotation rate. The second-order equations are then rewritten as

$$(\mathrm{D}/\mathrm{D}t)\langle u_i u_j\rangle + 2\epsilon_{ikp}\langle u_p u_j\rangle \Omega Ro^{-1} + 2\epsilon_{jkp}\langle u_p u_i\rangle \Omega_k Ro^{-1} = +\Pi_{ij}^r + \Pi_{ij}^s + \ldots,$$

$$(D/Dt)\langle \theta u_i\rangle + 2\epsilon_{pik}\Omega_k \langle \theta u_p\rangle Ro^{-1} = +\Pi_i^r + \Pi_i^s + \ldots,$$

where the terms omitted have already been given. Taking the contraction of the fourth-order tensor on the mean velocity gradients, to obtain the form used in the Reynolds stress equations, produces, with $q^2 = \langle u_p u_p \rangle$,

$$
\begin{aligned}
\Pi_{ij}^r/2q^2 = {} & 2[A_1 + A_2] S_{ij} \\
& + [(A_3 + A_4 + 2A_5)(b_{ip} S_{pj} + b_{jp} S_{pi}) + 2A_5 \delta_{ij} \langle bS \rangle] \\
& + [(A_3 - A_4)(b_{ip} W_{pj} + b_{jp} W_{pi})] \\
& + [(A_6 + A_7 + 2A_8)(b_{ip}^2 S_{pj} + b_{jp}^2 S_{pi}) + 2A_8 \delta_{ij} \langle b^2 S \rangle] \\
& + [(A_6 - A_7)(b_{ip}^2 W_{pj} + b_{jp}^2 W_{pi})] \\
& + 2[(A_9 + A_{10}) b_{ip} S_{pq} b_{qj} + A_{10} b_{ij} \langle bS \rangle] \\
& + [(A_{11} + A_{12} + 2A_{13})(b_{ip} S_{pq} b_{qj}^2 + b_{jp} S_{pq} b_{qi}^2) + 2A_{13}(b_{ij}^2 \langle bS \rangle + b_{ij} \langle b^2 S \rangle)] \\
& + [(A_{11} - A_{12})(b_{ip} W_{qp} b_{qj}^2 + b_{jp} W_{qp} b_{qi}^2)].
\end{aligned}
$$

Here the angle brackets represent the trace of the indicated quantity: e.g. $\langle bS \rangle = b_{ij} S_{ij}$ and $\mathrm{II} = -\frac{1}{2}\langle b^2 \rangle$, $\mathrm{III} = \frac{1}{3}\langle b^3 \rangle$. Note that the Π_{ij}^r has zero trace because of the continuity constraint, $X_{ijjk} = 0$, requires $A_3 + A_4 + 5A_5 - \mathrm{II}\,(A_{11} + A_{12} + 4A_{13}) = 0$ and $A_6 + A_7 + 5A_8 + A_9 + A_{10} = 0$.

It is possible to rewrite the higher-order tensor bases in terms of the lower-order terms, substantially simplifying the form of the model. The generalized Cayley–Hamilton theorem (Rivlin 1955) is used to rewrite the expression in an irreducible tensor basis (see Appendix C). Using the matrix notation

$$
\begin{aligned}
\boldsymbol{bSb} &= -[\boldsymbol{b}^2\boldsymbol{S} + \boldsymbol{Sb}^2] + \langle bS \rangle \boldsymbol{b} + \tfrac{1}{2}\langle b^2 \rangle \boldsymbol{S} + \langle b^2 S \rangle \boldsymbol{I}, \\
\boldsymbol{bSb}^2 + \boldsymbol{b}^2\boldsymbol{Sb} &= -\tfrac{1}{3}\langle b^3 \rangle \boldsymbol{S} + \langle b^2 S \rangle \boldsymbol{b} + \langle bS \rangle \boldsymbol{b}^2
\end{aligned}
$$

the 2DMFI rapid-pressure correlation can be written more compactly as

$$
\begin{aligned}
\Pi_{ij}^r/2q^2 = {} & [B_3 + \langle b^2 \rangle B_3'' + \langle b^3 \rangle B_3'''] S_{ij} \\
& + B_4[b_{ip} S_{pj} + b_{jp} S_{pi} - \tfrac{2}{3}\langle bS \rangle \delta_{ij}] + B_4''' \langle bS \rangle [b_{ij}^2 + 2\mathrm{II}/3\delta_{ij}] \\
& + B_5[b_{ip} W_{pj} + b_{jp} W_{pi}] + [B_6 \langle bS \rangle + B_4''' \langle b^2 S \rangle] b_{ij} \\
& + B_7[b_{ip}^2 S_{pj} + b_{jp}^2 S_{pi} - \tfrac{2}{3}\langle b^2 S \rangle \delta_{ij}] \\
& + B_8[b_{ip}^2 W_{pj} + b_{jp}^2 W_{pi}] + B_9[b_{ip} W_{qp} b_{qj}^2 + b_{jp} W_{qp} b_{qi}^2],
\end{aligned} \tag{38}
$$

where the values of the B_i in terms of the A_i are given in Appendix A. The above representation of the rapid-pressure correlation will be called the basic or uncalibrated model. The coefficients, B_i, appearing in the base 2DMFI model above come from first principles: they do not result from any numerical optimization with experimental or numerical data. Comparisons to the FLT model (Fu *et al.* 1987) shows that the two models have the same tensor structure containing the same generators. The only difference is that the terms proportional to $[b_{ij}]$ and $[b_{ij}^2 + 2\mathrm{II}/3\delta_{ij}]$, usually identified with the slow-pressure's contribution to the pressure–strain correlation and calibrated accordingly, now reflect a contribution from the rapid pressure. Contraction of the irreducible form of X_{ijkl} on the mean velocity gradients has produced the bases $[b_{ij}]$ and

$[b_{ij}^2+2\mathrm{II}/3\delta_{ij}]$ in which the coefficients are functions of the invariants $\langle bS\rangle$ and $\langle b^2S\rangle$ in addition to the dependence on $\langle b^2\rangle$ and $\langle b^3\rangle$ appearing in the A_i. The two tensor bases, usually associated with the slow-pressure correlation, arise as a consequence of starting with the two-point volume integral and represent a contribution to the pressure–strain correlation whose structure is identical to the slow-pressure models but whose genesis is in the rapid pressure.

Speziale *et al.* (1991) have written a general form for the pressure–strain covariance. It is linear in the mean velocity gradients and nonlinear in the anisotropy tensor. Their general expression contains the same generators as the present model except for the cubic term $[\boldsymbol{bWb^2-b^2Wb}]$. Speziale *et al.* (1991) have used the results from rational mechanics (cf. Smith 1971) to expand in a functional basis; here a polynomial basis has been used and in a polynomial representation the generator $[\boldsymbol{bWb^2-b^2Wb}]$ is not redundant (Spencer 1971). The tensor polynomial given above is irreducible and the basis is optimal. Speziale *et al.* (1991) have specialized the general expression to the case of planar flow: they have shown that the generators nonlinear in the anisotropy tensor can be expressed in terms linear in the anisotropy tensor. This fact led to the very simple form of the SSG model (Speziale *et al.* 1991), and also, from a rigorous though not necessarily practical point of view, limits the model to planar flows. The results of Speziale *et al.* (1991) can also be used to recast the present model into its linear planar form. For planar flows Speziale *et al.* (1991) have shown that

$$[b_{ip}^2 S_{pj}+b_{jp}^2 S_{pi}-\tfrac{2}{3}\langle b^2S\rangle\,\delta_{ij}] = -b_{33}[b_{ip}S_{pj}+b_{jp}S_{pi}-\tfrac{2}{3}\langle bS\rangle\,\delta_{ij}]-\tfrac{2}{3}(\mathrm{III}/b_{33})\,S_{ij},$$

$$[b_{ip}^2 W_{pj}+b_{jp}^2 W_{pi}] = -b_{33}[b_{ip}W_{pj}+b_{jp}W_{pi}],$$

from which it follows that

$$[b_{ip}W_{qp}b_{qj}^2+b_{jp}W_{qp}b_{qi}^2] = (\mathrm{II}+b_{33}b_{33})[b_{ip}W_{pj}+b_{jp}W_{pi}]$$

and the planar form of the 2DMFI rapid-pressure model can be written as

$$\begin{aligned}\Pi_{ij}^r/2q^2 = {} & (C_3-2\mathrm{II}C_3''+3\mathrm{III}C_3'''-\tfrac{2}{3}(\mathrm{III}/b_{33})\,C_7)\,S_{ij}\\ & +(C_4-b_{33}C_7)[b_{ip}S_{pj}+b_{jp}S_{pi}-\tfrac{2}{3}\langle bS\rangle\,\delta_{ij}]\\ & +C_4'''\langle bS\rangle[b_{ij}^2+2\mathrm{II}/3\delta_{ij}]\\ & +(C_5-b_{33}C_8+(\mathrm{II}+b_{33}b_{33})C_9)[b_{ip}W_{pj}+b_{jp}W_{pi}]\\ & +(C_6\langle bS\rangle+C_4'''\langle b^2S\rangle)\,b_{ij},\end{aligned} \tag{39}$$

which has the same linear tensor bases as the SSG model, in which the slow-pressure covariance is included:

$$\begin{aligned}\Pi_{ij}^r = {} & -(2C_1\epsilon+C_1^*\mathscr{P})\,b_{ij}+C_2\epsilon[b_{ij}^2+2\mathrm{II}/3\delta_{ij}]+(C_3-(-2\mathrm{II})^{1/2}C_3^*)\,kS_{ij}\\ & +C_4k[b_{ip}S_{pj}+b_{jp}S_{pi}-\tfrac{2}{3}\langle bS\rangle\,\delta_{ij}]+C_5k[b_{ip}W_{pj}+b_{jp}W_{pi}].\end{aligned} \tag{40}$$

In the planar flow limit the form of the two models is the same. This is to be expected as both derivations begin with the topologically generic form of a general class of models linear in the mean flow gradients and satisfying form invariance under coordinate transformation; the SSG model is a specialization of this form to planar flows. There are some additional differences worth noting. The coefficients in the basic form of the 2DMFI model are nonlinear functions of the invariants while in the SSG model the coefficients are, except for the S_{ij} term, constants. The constants in the SSG

model come from calibration to several equilibrium flows and may be viewed as the zeroth-order term in a Taylor series expansion of the variable coefficients. The C_i in the SSG model are determined by a numerical optimization so that the model reproduces as closely as possible: (i) the stationary state of the homogeneous shear and (ii) maximizes the kinetic energy growth rate of the rotating homogeneous shear to as close as possible to the $\Omega/S = 0.25$ predicted by rapid distortion theory without introducing a Richardson number similarity (Speziale & Mhuiris 1989*a*), while ensuring that the points of exchange of stability are outside those predicted by the linear theory of Bertoglio (1982). Issues regarding constant-coefficient models are discussed in more detail in §10.

In the return term of the SSG model the correction to the linear b_{ij} term arrived at more or less intuitively by Speziale *et al.* (1991) is, to lowest order, vindicated by the present results. Speziale *et al.* (1991) have altered the term linear in b_{ij}, usually associated with the slow-pressure correlation, to include a term involving the mean flow, a term proportional to the production $\mathscr{P} = -\langle u_i u_j \rangle U_{i,j}$: the usual

$$C_1 \epsilon b_{ij} \rightarrow (C_1 \epsilon + C_1^* \mathscr{P}) b_{ij}.$$

The present analysis indicates that the portion of the rapid-pressure contribution to the pressure–strain correlation, linear in b_{ij}, has the form $[B_6 \langle bS \rangle + B_4''' \langle b^2 S \rangle] b_{ij}$. Note that $\langle bS \rangle$ can be written in terms of the production as $\langle bS \rangle = -\mathscr{P}/q^2$. The present analysis suggests the possibility of adjusting the nonlinear return term for mean velocity gradient effects in a similar way. In the present model the portion of the rapid-pressure quadratic in the anisotropy tensor is $B_4''' \langle bS \rangle [b_{ij}^2 + 2II/3\delta_{ij}]$ and therefore also scales with the production. Speziale, Gatski & Sarkar (1992) have reflected on the ambiguity of the distinction between the rapid- and slow-pressure contributions to the pressure–strain correlation. They have modelled the whole pressure–strain correlation, but whether to interpret their adjustments (as described in the previous paragraph) as incorporating the effects of the mean strain on the return terms or as contributions of the rapid pressure to the total pressure–strain is not clear. Here, however, the distinction is clear. The present analysis starts from the tensor polynomial representation for the rapid-pressure integral and produces terms whose tensor structure is identical to that for terms which are traditionally called the slow pressure. The other nonlinear pressure–strain models, FLT or the SL model (Shih & Lumley 1985), do not have terms in b_{ij} or b_{ij}^2 that can be similarly identified.

The derivation of a rapid-pressure covariance representation consistent with the extreme states and valid away from these limit states, though mathematically rigorous, will not necessarily produce a model that performs better than other models in flows for which latter models are calibrated. However, for the general class of flows for which second-order models are suitable we are of the opinion that the satisfaction of all mathematical constraints constitutes a necessary (though not sufficient) requirement to ensure the predictive capabilities in flows different from those for which the models are calibrated. The existence of several free parameters can then be used to calibrate the model to specific classes of flows of computational interest. This tack is taken in the next section where the fixed points of the modelled equation are matched to the fixed points of the homogeneous shear. In this way a model for the class of flows in which the mean shear is the dominant production mechanism is created.

8. Calibrating the rapid-pressure covariance representation

The coefficients, B_i, appearing in the 2DMFI model come from first principles: they do not result from any calibration with experimental or numerical data. They represent the minimum number of determined coefficients necessary to satisfy all the mathematical constraints on the rapid-pressure correlation for an arbitrary Reynolds stress. It is not, however, a unique representation: there are an infinity of solutions corresponding to different values of the free parameters which, in the basic model representation shown above, have been set to zero. Computations have shown that the predictive capabilities of the basic model are inadequate. The mathematics built into the model do not capture the experimentally known 'stationary points' of homogeneous shear. To compensate for some of the approximations made in the mathematical development the model is modified so that the modelled evolution equations have the same asymptotic behaviour as that observed in nature. Additional terms are added to the basic model to ensure that it is consistent with an equilibrium state of a particular benchmark turbulent field, homogeneous shear. This is done without sacrificing any of the mathematical principles built into the model. However, it cannot be done arbitrarily.

The strategy is to require asymptotic consistency with an equilibrium state. There is some reason to believe that the assumption of an equilibrium fixed-point behaviour is a suitable approximation for turbulent flows of the sort for which this modelling procedure is useful. Experiments in homogeneous shear flow show that the structural equilibrium point, $(\mathrm{D}/\mathrm{D}t)\,b_{ij} = 0$ is a weak function of $\mathscr{P}/\epsilon$ and also the initial conditions. Here it is assumed that fixed-point behaviour is an adequate approximation for use in calibration for engineering computations. Thus the modelled evolution equations are required to have the same fixed points as those observed in experiment. The equilibrium constraint is used to obtain additional constraints equations to specify the free parameters. This is very similar to the strategy employed so far in that limit states are used to set model coefficients. Here, of course, the 'equilibrium' state is much closer to those expected to be seen in flows of engineering interest. The free parameters will now be called calibration coefficients, A_i^c, and will be collectively denoted by X^{∞}_{ijkl} appearing in the decomposition

$$X_{ijkl} = X^{0}_{ijkl} + FX^{F}_{ijkl} + FX^{\infty}_{ijkl}. \tag{41}$$

X^{∞}_{ijkl} represents the additional constant terms necessary to capture the stationary state. This form is equivalent to assuming that the coefficients in the tensor polynomial have the form $A_i = A_i^0 + FA_i^F + FA_i^c$. The A_i^c satisfy normalization and continuity constraints and the algebraic equations for the fixed point of the homogeneous shear. It is at this point that numerical or experimental data for the asymptotic values of the anisotropy tenor, the production to dissipation, $(\mathscr{P}/\epsilon)_{\infty}$, and the ratio of timescales, $(Sk/\epsilon)_{\infty}$, are necessary. The details of this strategy are now given.

The A_i^c satisfy the six equations given by the homogeneous form of normalization and continuity constraints, $X^{\infty}_{ijkk} = 0, X^{\infty}_{ijjk} = 0$, which are valid for all states of the turbulence. Substituting in the calibration coefficients allows six A_i^c to be expressed in terms of seven free parameters:

$$\begin{aligned}
A_1^c &= -(50A_8^c + 12A_9^c + 4A_{10}^c)\,\mathrm{II}/15 + (A_{11}^c + A_{12}^c - 6A_{13})\,\mathrm{III}/5,\\
A_2^c &= (20A_8^c + 3A_9^c + A_{10}^c)\,\mathrm{II}/15 - (3A_{11}^c + 3A_{12}^c + 2A_{13})\,\mathrm{III}/10,\\
A_3^c &= -\tfrac{11}{3}A_5^c + (A_{11}^c + 3A_{12}^c + 8A_{13}^c)\,\mathrm{II}/3, \quad A_4^c = -\tfrac{4}{3}A_5^c + 2(A_{11}^c + 2A_{13}^c)\,\mathrm{II}/3,\\
A_6^c &= -\tfrac{1}{3}(11A_8^c + 3A_9^c + A_{10}^c), \quad A_7^c = -\tfrac{2}{3}(2A_8^c + A_{10}^c).
\end{aligned}$$

The seven parameters will be determined by requiring asymptotic consistency with a particular equilibrium state. At this point the rapid-pressure correlation model is fully general and it is possible to write it in its final form, without specifying the calibration coefficients, as

$$\begin{aligned}\Pi^r_{ij}/2q^2 = {} & [C_3 - 2\mathrm{II}C_3'' + 3\mathrm{III}C_3''']\,S_{ij} \\ & + C_4[b_{ip}S_{pj} + b_{jp}S_{pi} - \tfrac{2}{3}\langle bS\rangle\delta_{ij}] + C_4'''\langle bS\rangle[b^2_{ij} + 2\mathrm{II}/3\delta_{ij}] \\ & + C_5[b_{ip}W_{pj} + b_{jp}W_{pi}] + [C_6\langle bS\rangle + C_4'''\langle b^2S\rangle]\,b_{ij} \\ & + C_7[b^2_{ip}S_{pj} + b^2_{jp}S_{pi} - \tfrac{2}{3}\langle b^2S\rangle\delta_{ij}] \\ & + C_8[b^2_{ip}W_{pj} + b^2_{jp}W_{pi}] + C_9[b_{ip}W_{qp}b^2_{qj} + b_{jp}W_{qp}b^2_{qi}]. \end{aligned} \tag{42}$$

The calibration coefficients, A^c_i, are added to the base model coefficients, B_i, of the previous section, to obtain the final model coefficients C_i:

$$\begin{aligned} C_3 &= B_3 - 2F(10A^c_8 + 3A^c_9 + A^c_{10})\,\mathrm{II}/5 - F(A^c_{11} + A^c_{12} + 14A^c_{13})\,\mathrm{III}/5, \\ C_3'' &= B_3'' + F(A^c_9 + A^c_{10}), \quad C_3''' = B_3''' - \tfrac{1}{3}F(A^c_{11} + A^c_{12} + 2A^c_{13}), \\ C_4 &= B_4 + F(-3A^c_5 + \mathrm{II}(A^c_{11} + A^c_{12} + 4A^c_{13})), \quad C_4''' = B_4''' + F(A^c_{11} + A^c_{12} + 4A^c_{13}), \\ C_5 &= B_5 + F(-\tfrac{7}{3}A^c_5 + \tfrac{1}{3}\mathrm{II}(-A^c_{11} + 3A^c_{12} + 4A^c_{13})), \\ C_6 &= B_6 + F(2A^c_9 + 4A^c_{10}), \quad C_7 = B_7 - 3F(A^c_8 + A^c_9 + A^c_{10}), \\ C_8 &= B_8 - \tfrac{1}{3}F(7A^c_8 + 3A^c_9 - A^c_{10}), \quad C_9 = B_9 + F(A^c_{11} - A^c_{12}). \end{aligned}$$

Note that the traces can be written in terms of the production $\langle bS\rangle = -\mathscr{P}/q^2$ and $\langle b^2S\rangle = \frac{1}{2}b_{33}\mathscr{P}/q^2$; in planar flow $\langle bS\rangle = -2b_{12}S$ and $\langle b^2S\rangle = -b_{12}b_{33}\mathscr{P}/q^2$.

The calibration coefficient A^c_5 involves adjustments to the generators

$$[\boldsymbol{bS} + \boldsymbol{Sb} - \tfrac{2}{3}\langle bS\rangle\boldsymbol{I}] \quad \text{and} \quad [\boldsymbol{bW} - \boldsymbol{Wb}]$$

which are linear in the anisotropy tensor. Numerical experiments have indicated that it is important in establishing the levels of the normal components of the Reynolds stresses. Combinations of A^c_8, A^c_9 and A^c_{10} affect the generators quadratic in the anisotropy tensor, $[\boldsymbol{b^2S} + \boldsymbol{b^2S} - \frac{2}{3}\langle b^2S\rangle\boldsymbol{I}]$ and $[\boldsymbol{b^2W} - \boldsymbol{Wb^2}]$ and to a very small degree the $\boldsymbol{S}$-term. Combinations of only A^c_9 and A^c_{10} can be used to control the contribution to Π^r proportional to $\boldsymbol{b}$ and $\boldsymbol{S}$. Experience with the FLT model (Fu *et al.* 1987) indicates that the cubic term $[\boldsymbol{bWb^2} - \boldsymbol{b^2Wb}]$ involving the rotation tensor is important in controlling the relative level of the normal components of the Reynolds stress in situations with rotation. This suggests that the calibration coefficients A^c_{11}, A^c_{12} and A^c_{13} are important. The combination of calibration coefficients A^c_{11} and A^c_{12} controls tensor products like $[\boldsymbol{bWb^2} - \boldsymbol{b^2Wb}]$ and combination of terms A^c_{11}, A^c_{12} and A^c_{13} control the contributions of $\boldsymbol{b^2}$ and $\boldsymbol{S}$.

The existence of the free parameters allows the model to be calibrated to a specific class of flows of computational interest. For example, in a buoyant flow one might evaluate the fixed points using experiments on homogeneous shear in a constant mean temperature gradient, thus producing a model suitable for a class of stratified flows of geophysical interest. This calibration would, of course, involve the model for the rapid-pressure correlation appearing in the heat-flux equation. For many engineering problems the primary production mechanism is the mean shear and capturing the fixed points of the homogeneous shear in the modelled equations will make the model suitable for a wide class of flows. At this point one could also consider using the exact results of rapid-distortion theory to obtain values for the calibration coefficients. This,

	TC	CHC	TK(A)	TK(C)	TK(D)	TK(G)	TK(J)	TK(K)	DNS
b_{11}^{∞}	0.197	0.137	0.217	0.257	0.197	0.157	0.157	0.147	0.215
b_{12}^{∞}	−0.14	−0.165	−0.165	−0.165	−0.17	−0.148	−0.154	−0.149	−0.158
b_{22}^{∞}	−0.143	−0.083	−0.133	−0.143	−0.133	−0.113	−0.103	−0.093	−0.153
b_{33}^{∞}	−0.053	−0.053	−0.083	−0.113	−0.063	−0.043	−0.053	−0.053	−0.062
$(\mathscr{P}/\epsilon)_{\infty}$	1.75	1.0	1.38	1.37	1.64	1.33	1.45	1.37	1.80
$(SK/\epsilon)_{\infty}$	6.25	3.03	4.2	4.15	4.82	4.5	4.71	4.60	5.7

TABLE 1. Data for homogeneous shear flow from Tavoularis & Corrsin (1981) (TC), Champagne *et al.* (1970) (CHC), Tavoularis & Karnik (1989) (TK) and DNS data of Rogers *et al.* (1986).

however, is inconsistent with the equilibrium hypothesis underlying the local approximation to the constitutive relation invoked for the rapid-pressure correlation integral. Furthermore the modelled dissipation equation assumes that the small scales are parameterizable by the large scales, acting to dissipate turbulent kinetic energy at a rate set of the flux from the large scales. The rapid problem distorts the small scales of the motion causing them to evolve dynamically in a way that is no longer set by the spectral cascade and they are no longer parameterizable by the large scales of the motion. It is this apparent limitation of the current class of modelled dissipation equations that underlies the choice not to use RDT to calibrate the representation. The structural equilibrium homogeneous shear will be used to fix the representation for the rapid-pressure correlation.

The fixed points of the homogeneous shear are now built into the model by specifying the calibration coefficients. The modelled evolution equations for the Reynolds stresses in a homogeneous turbulence with a mean velocity gradient,

$$(\mathrm{D}/\mathrm{D}t)\langle u_i u_j\rangle = -2\epsilon_{ikp}\langle u_p u_j\rangle \Omega_k - 2\epsilon_{jkp}\langle u_p u_i\rangle \Omega_k - \langle u_i u_p\rangle U_{j,p} - \langle u_j u_p\rangle U_{i,p} + \Pi_{ij}^{r} - C_1 \epsilon b_{ij} + C_2 \epsilon[b_{ij}^2 + 2\mathrm{II}/3\delta_{ij}] - 2/3\epsilon\delta_{ij}, \quad (43)$$

assuming local isotropy for the dissipation. The terms $-C_1\epsilon b_{ij} + C_2\epsilon[b_{ij}^2 + 2\mathrm{II}/3\delta_{ij}]$ represent the return-to-isotropy pressure correlation. Using $\langle u_i u_j\rangle = q^2(b_{ij} + 1/3\delta_{ij})$ the equations for the anisotropy are

$$(\mathrm{D}/\mathrm{D}t)\, b_{ij} = -2\epsilon_{ikp} b_{pj}\Omega_k - 2\epsilon_{jkp} b_{pi}\Omega_k - [b_{ip} U_{j,p} + b_{jp} U_{i,p} - 2/3\delta_{ij}\langle bS\rangle] - 2/3 S_{ij} + 2b_{ij}\langle bS\rangle + \Pi_{ij}^{r}/q^2 - (C_1 - 2)\, b_{ij}\epsilon/q^2 + C_2[b_{ij}^2 + 2\mathrm{II}/3\delta_{ij}]\epsilon/q^2. \quad (44)$$

The mean strain and rotation tensors are

$$S_{ij} = \tfrac{1}{2}S^*(\delta_{i1}\delta_{j2} + \delta_{i2}\delta_{j1}) \quad \text{and} \quad W_{ij} = \tfrac{1}{2}W^*(\delta_{i1}\delta_{j2} - \delta_{i2}\delta_{j1}),$$

where, $S = U_{1,2} = S^* = W^*$. Setting the $(\mathrm{D}/\mathrm{D}t)\, b_{ij} = 0$ produces three algebraic equations. Inserting the experimentally determined asymptotic values of b_{ij} and Sk/ϵ produces three additional constraints leaving four of the seven A_i^c as free parameters. The data from the experiments of Tavoularis & Corrsin (1981), Champagne, Harris & Corrsin (1970), Tavoularis & Karnik (1989), and the DNS of Rogers, Moin & Reynolds (1986) are summarized in table 1.

There is considerable scatter in the data due to the techniques used to generate the turbulence, individual wind tunnels in which the different experiments were done, and experimental error. Not all the data, as has been qualified in the references from which the data is drawn, represent the asymptotic state. The following fixed-point values are taken to be representative: $b_{11}^{\infty} = 0.203$, $b_{12}^{\infty} = -0.156$, $b_{22}^{\infty} = -0.143$, $b_{33}^{\infty} = -0.06$, $(Sk/\epsilon)_{\infty} = 5.54$, $(\mathscr{P}/\epsilon)_{\infty} = 1.73$. They are obtained by a simple average of the data of

Tavoularis & Corrsin, Tavoularis & Karnik and Rogers *et al.* These three cases are chosen because they have the highest values of the non-dimensional time $(SK/\epsilon)_\infty$, corresponding to flows that are furthest in their development to the asymptotic state. The values of the invariants corresponding to these values of the anisotropy tensor are: $\mathrm{II}_\infty = -0.058$, $\mathrm{III}_\infty = 0.0032$, $F_\infty = 0.574$. Substituting these asymptotic values into the fixed-point equations, $(\mathrm{D}/\mathrm{D}t)\, b_{ij} = 0$, reduces the number of free parameters from seven to four:

$$A_5^c = -0.29 + 0.06(A_{10}^c - A_8^c),$$
$$A_{11}^c = -3.6 + 5A_{10}^c - 2A_{13}^c - 12.7A_8^c - 3.8A_9^c,$$
$$A_{12}^c = -24.5 - 44.8A_{10}^c - 2A_{13}^c + 28.7A_8^c - 8.65A_9^c.$$

This set of constraint equations is dependent on the model for the return-to-isotropy pressure but not the dissipation equation. In Appendix B a set of equations is given so that the modelling can be done for any return term. For simplicity the nonlinear return coefficient has been set to zero, $C_2 = 0$, and the well-accepted value, $C_1^\infty = 3.4$, has been chosen. There are still four free parameters, for which the following values are chosen: $A_8^c = 0.6$, $A_9^c = -0.6$, $A_{10}^c = -0.15$, $A_{13}^c = 0$. The undetermined free parameters have been set by matching the values of the anisotropy for the log layer. The procedure is outlined in more detail in Appendices A and B.

9. Computations and comparisons for homogeneous turbulence

The 2DMFI model falls into the same class of representations as the FLT (Fu *et al.* 1987) and SL (Shih & Lumley 1985) models: they all use nonlinear terms and invoke some form of realizability constraint to evaluate the coefficients. For this reason the 2DMFI model will be compared primarily to the nonlinear SL and FLT models. For completeness and because it appears to be a very successful model for planar flows, computations with the quasi-linear SSG model (Speziale *et al.* 1991) are also shown. The SSG model is linear in the anisotropy tensor though nonlinear in that the scalar coefficients are functions of the invariants of the anisotropy tensor. It should, however, be kept in mind that the SSG model satisfies realizability for the kinetic energy and not for the individual Reynolds stresses and is therefore in another class of models. This issue is more fully explored in §10. Results are not compared to the LRR model (Launder, Reece & Rodi 1975) as, in concordance with the observations of Speziale *et al.* (1991), the SSG model is viewed as an updated optimized LRR model. Detailed forms of these models are given in Appendix D.

In all the calculations with the 2DMFI model a simple linear Rotta-type model for the slow-pressure correlation will be used. This corresponds to $C_2 = 0$ in the canonical form given above and is consistent with the present calibration to the homogeneous shear. For the linear return coefficient a simple expression, $C_1 = 2 - 31\mathrm{II}F^{1/2}$, is used. This satisfies the isotropic limit, $C_1 = 2.0$, and is consistent with the assumed value for the asymptotic homogeneous shear, $C_1^\infty = 3.4$. The form chosen is consistent with the weak form of realizability of Speziale *et al.* (1994) which requires that the rapid-pressure correlation vanish more rapidly than the return pressure correlation as the realizability limit is approached. The dissipation equation used is

$$(\mathrm{D}/\mathrm{D}t)\,\epsilon = -(C_{\epsilon 1}\langle u_i u_j\rangle U_{i,j} + C_{\epsilon 2}\,\epsilon)\,\epsilon/k. \tag{45}$$

The values used for the constants are: $C_{\epsilon 1} = 1.44$, $C_{\epsilon 2} = 1.83$. Note that this corresponds to a single universal fixed point $(\mathscr{P}/\epsilon)_\infty = 1.88$ independent of rotation. This single fixed point is a well-known deficiency common to all the present forms of the modelled dissipation equation.

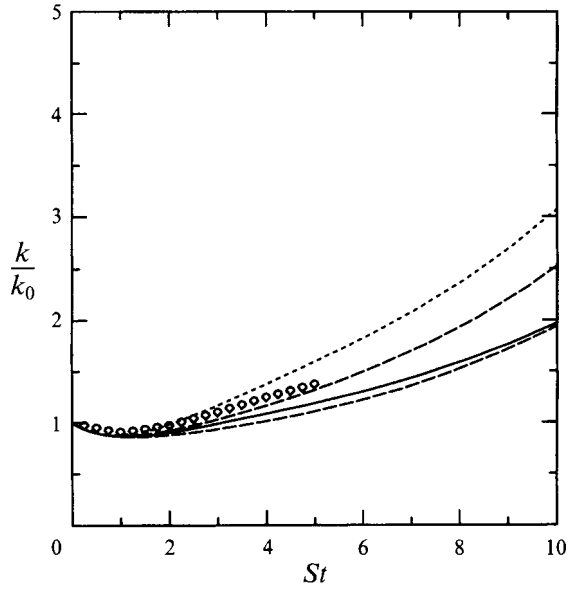

FIGURE 1. Evolution of the kinetic energy in homogeneous shear. The experiments of Bardina *et al.* (1983) (symbols) are compared to the four different models: ——, 2DMFI; – – –, SL; - - - - -, FLT; and ———, SSG.

Equilibrium values	2DMFI model	SL model	FLT model	SSG model	Experimental data
b_{11}^{∞}	0.209	0.202	0.208	0.219	0.203
b_{12}^{∞}	−0.155	−0.080	−0.146	−0.164	−0.156
b_{22}^{∞}	−0.148	−0.195	−0.144	−0.146	−0.143
b_{33}^{∞}	−0.061	0.007	−0.064	−0.073	−0.06
$(\mathscr{P}/\epsilon)_{\infty}$	1.88	3.42	1.99	1.88	1.73
$(SK/\epsilon)_{\infty}$	6.08	21.35	6.84	5.76	5.54

TABLE 2. Comparison of the model predictions for the equilibrium values in homogeneous shear flow ($\mathscr{P}/\epsilon = 1.88$) with an average of the experimental data.

Case 1. *Homogeneous shear*

The calibrated model is now used to compute the time evolution of homogeneous shear flow. The mean strain and rotation tensors are $S_{ij} = \frac{1}{2}S^*\ (\delta_{i1}\delta_{j2} + \delta_{i2}\delta_{j1})$ and $W_{ij} = \frac{1}{2}W^*(\delta_{i1}\delta_{j2} - \delta_{i2}\delta_{j1})$, where $S = U_{1,2} = S^* = W^*$. In figure 1 the time evolution of the turbulence energy is compared to the LES of Bardina, Ferziger & Reynolds (1983), and the three models FLT, SL and SSG. A similar monotonic behaviour is found for other statistics, b_{12}, b_{11}, II in the flow and, as they do not constitute new or different information, are not shown. In general, starting from physically realistic initial conditions, the flow attains its asymptotic state rapidly and monotonically. The asymptotic states which the different models predict are given in table 2. The column labelled experimental data is an average of the three cases TC, DNS and TK(D). Note that the different $(\mathscr{P}/\epsilon)_{\infty}$ attained are functions of the different $C_{\epsilon 1}$ and $C_{\epsilon 2}$ used in the models. The present form of the dissipation equation ensures that the quantity $(\mathscr{P}/\epsilon)_{\infty} = 1.88$ regardless of initial conditions for all Sk/ϵ. This is a shortcoming of the

Equilibrium values	2DMFI model	SL model	FLT model	SSG model	DNS data	Experimental data
b_{11}^{∞}	0.176	0.079	0.141	0.201	0.180	0.22
b_{12}^{∞}	−0.144	−0.116	−0.162	−0.160	−0.134	−0.16
b_{22}^{∞}	−0.136	−0.082	−0.099	−0.127	−0.140	−0.143
b_{33}^{∞}	−0.039	0.003	−0.042	−0.074	−0.040	−0.06
$(\mathscr{P}/\epsilon)_{\infty}$	1.0	1.0	1.0	1.0	1.0	1.0
$(SK/\epsilon)_{\infty}$	3.46	4.30	3.09	3.12	3.73	3.1

TABLE 3. Comparison of the model predictions for the equilibrium values in the log-layer of turbulent channel flow ($\mathscr{P}/\epsilon = 1$) with the DNS data of Kim (1993, personal communication) and the data of Laufer (1951) given in Abid & Speziale (1993).

modelled dissipation equation and shows up in a larger b_{11} than for the flow for which the rapid-pressure representation was calibrated using $(\mathscr{P}/\epsilon)_{\infty} = 1.73$. Recall that the calibration of the model was done using stationary flows and as such the calibration is independent of the dissipation equation model. The slower evolution of the kinetic energy also reflects the larger source term for the dissipation in the dissipation equation.

Case 2. *The equilibrium wall layer*

Another simple but important test case is whether the model can capture the stationary state of the log-layer in channel flow. Homogeneous shear and the log-layer are similar in that they achieve, to a suitable approximation, an equilibrium state. Note that the dissipation equation is not used to compute this flow as $\mathscr{P} = \epsilon$. Abid & Speziale (1993) have discussed the relevance of this test case and noted the inability of most rapid-pressure closures to perform successfully in the log-layer. The results are in agreement with their contention that a model which is asymptotically consistent with the stationary states of the homogeneous shear will also do well in the log-layer. The models are compared to the channel flow DNS of J. Kim (1993, personal communication) which is an update of the simulations reported in Kim, Moin & Moser (1987), table 3. The data presented represent an average of the values of the anisotropy in the region $70 \leqslant y^{+} \leqslant 100$ outside the viscous sublayer.

Case 3. *Homogeneous shear with rotation*

The present test case, homogeneous shear with rotation, and the next test case, homogeneous shear with streamline curvature, are important. In both, additional forces, which stabilize or destabilize the flow, are present. These effects appear in the evolution equations as additional production mechanisms for the Reynolds stresses. In the case of rotation the production terms in the evolution equation for the turbulence kinetic energy do not directly depend on the rotation: the turbulence energy production depends on the rotation only through the off-diagonal components of the Reynolds stress. On the other hand, in the case of streamline curvature the production terms in the evolution equation of the turbulence kinetic energy do directly depend on the curvature. These two cases are important test cases not only because the models have not been calibrated for them but also because the model will have to predict both the stabilization and destabilization of the turbulence and the critical values of the governing parameters which demarcate the regions of flow stabilization from flow destabilization.

For flows in the rotating coordinate system the Coriolis terms must be carried and

W_{ij} appearing in Π^r_{ij} must be replaced by the total rotation tensor $W_{ij}+\epsilon_{jik}\Omega_k$. Thus in the rapid-pressure model $W^* = S(1-2\Omega/S)$.

Figure 2(*b–e*) shows how the models perform in rotating shear for rotation to shear ratios $\Omega/S = 0, \frac{1}{4}, \frac{1}{2}$ compared to the LES data of Bardina *et al.* (1983) in figure 2(*a*). In general, all the models are able to capture both flow destabilization for some $A \leqslant \Omega/S \leqslant B$ and flow stabilization for some $A > \Omega/S > B$. The points A and B represent the points of neutral stability on a bifurcation diagram in the phase plane $(\epsilon/Sk)_\infty$ and $(\Omega/S)_\infty$. All of the models have a bifurcation diagram of the same general form (Speziale & Mhuiris 1989*b*), indicating a stabilization of the flow outside some region of approximate size $0 \leqslant \Omega/S \leqslant 0.5$, predicted by the linear rapid-distortion theory of Bertoglio (1982). The most important facts concerning the different models for the homogeneous rotating shear can be summarized by indicating the unstable regions in which the models predict a non-trivial equilibrium $(\epsilon/Sk)_\infty$:

$$\begin{aligned} \text{SSG:} \quad & -0.09 \leqslant \Omega/S \leqslant 0.53, \\ \text{RDT:} \quad & 0.00 \leqslant \Omega/S \leqslant 0.50, \\ \text{2DMFI:} \quad & -0.070 \leqslant \Omega/S \leqslant 0.502, \\ \text{SL:} \quad & -0.14 \leqslant \Omega/S \leqslant 0.40, \\ \text{FLT:} \quad & -0.11 \leqslant \Omega/S \leqslant 0.39. \end{aligned}$$

Near the point of linear neutral stability $\Omega/S = 1/2$ both the SL and the FLT models predict a premature restabilization at values of Ω/S 20% and 22% lower than predicted by the linear theory. The 2DMFI model is within 4% of the linear prediction.

None of the models tested, linear or nonlinear, captures the point of maximum kinetic energy growth at $(\Omega/S)_{max} = 0.25$. To do so would mean that the equations would exhibit a Richardson number similarity which, as Speziale & Mhuiris (1989*a*) have shown, is not admitted by the Navier–Stokes equations. The two models that come closest to $(\Omega/S)_{max} = 0.25$ are SSG at $\Omega/S = 0.22$, which was calibrated using this fact, and 2DMFI at $\Omega/S = 0.2$ which was not calibrated using any rotating flows. The current modelled dissipation equations predict a $(\mathscr{P}/\epsilon)_\infty \equiv -2b_{12}Sk/\epsilon = (C_{\epsilon 2}-1)/(C_{\epsilon 1}-1) = \text{const.}$, where the constant is model dependent but independent of rotation rate. The constant attains the value for equilibrium homogeneous shear for arbitrary rotation rate, a fact which is not consistent with observation. In a flow that is stabilized by rotation, say $\Omega/S = 1$, production must be less than dissipation for the equilibrium state to be reached. The dissipation equation cannot be used for calibration in rotating flows without compromising the model when a dissipation equation capable of predicting the stationary values of $(\mathscr{P}/\epsilon)_\infty = f(\Omega/S)$ becomes available.

Case 4. Homogeneous shear with curvature

For homogeneous shear with streamline curvature the mean strain and rotation tensors are $S_{ij} = \frac{1}{2}S^*(\delta_{i1}\delta_{j2}+\delta_{i2}\delta_{j1})$ and $W_{ij} = \frac{1}{2}W^*(\delta_{i1}\delta_{j2}-\delta_{i2}\delta_{j1})$ where $S^* = S(1-\mathscr{S})$ and $W^* = S(1+\mathscr{S})$ where $\mathscr{S} = (U_c/R_c)/S$ is the stability parameter. The geometry for the curved homogeneous shear follows that of Holloway & Tavoularis (1992): R_c is the radius of curvature of the flow, U_c is the axial velocity at the centreline and the cross-stream gradient of the axial velocity is the shear $U_{1,2} = S$. The kinetic energy growth rate is suppressed, relative to homogeneous shear, for $\mathscr{S} > 0$ and increased for $\mathscr{S} < 0$, while for $\mathscr{S} > 0.05$ the experimental data indicate a relaminarization.

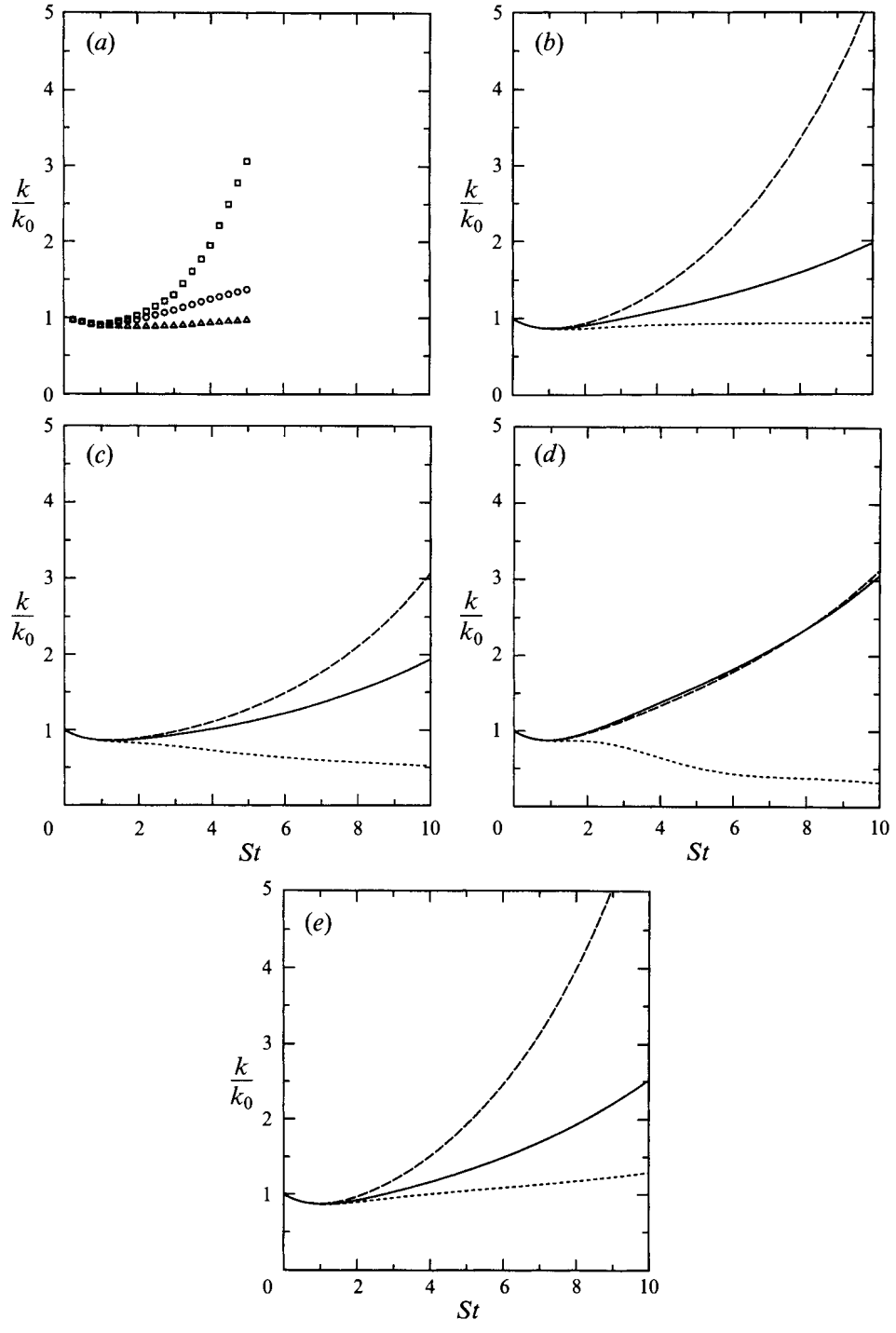

FIGURE 2. Evolution of the kinetic energy in homogeneous shear with rotation for (*a*) Bardina *et al.* (1981), (*b*) 2DMFI, (*c*) SL, (*d*) FLT, and (*e*) SSG. In ○, ——, $\Omega/S = 0$; □, — — —, 0.25; △, - - - - -, 0.5.

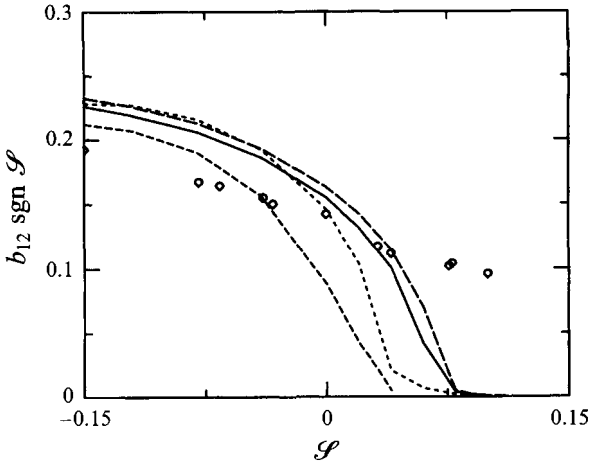

FIGURE 3. Off-diagonal component of the anisotropy tensor as a function of the stability parameter for homogeneous shear with streamline curvature: ——, 2DMFI; — — —, SSG; – –, SL; - - - - -, FLT. Experimental data of Holloway & Tavoularis (1992) are also shown (symbols).

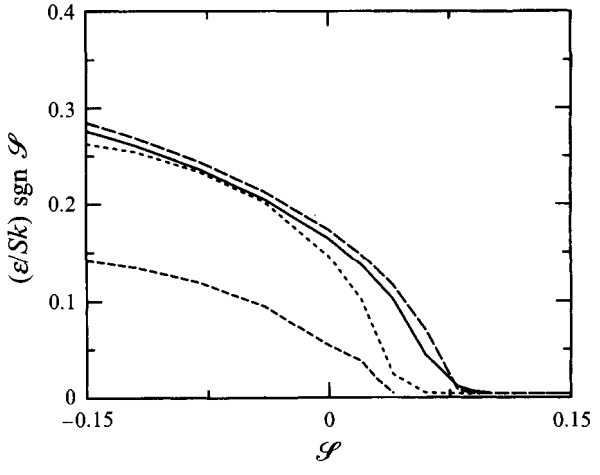

FIGURE 4. Bifurcation diagram for homogeneous shear with curvature for the four different models: ——, 2DMFI; — — —, SSG; – –, SL, - - - - -, FLT.

Figure 3 compares the model results to the experimental data for b_{12} versus $\mathscr{S}$. The plot has been generated by computing the flow from the beginning of the straight section of the wind tunnel to $St = 10$ which corresponds to the end of the curved section. The initial conditions on the second-order moments are given by the experimental data. The initial condition on the dissipation rate is determined by matching to the kinetic energy growth rate at the beginning of the straight section.

The different models all capture the trend in the stabilization/destabilization with respect to the stability parameter. The primary difference in the predictions of the different models seems related to their ability to capture the homogeneous shear at $\mathscr{S} = 0$. The results of the different models would be in more agreement for negative and small positive values of $\mathscr{S}$ if they predicted the same results for homogeneous shear.

The bifurcation diagram for the second-order models, in figure 4, was generated by letting the solution procedure go to its asymptotic state. There is a critical value, $\mathscr{S}_c$,

at which the stabilizing effects of curvature begins to causes a negative kinetic energy growth rate, which ultimately relaminarizes the flow. The critical values predicted by the different models, are

$$\begin{aligned} \text{H\&T:} \quad & \mathscr{S}_c = 0.05, \\ \text{2DMFI:} \quad & \mathscr{S}_c = 0.072, \\ \text{FLT:} \quad & \mathscr{S}_c = 0.075, \\ \text{SSG:} \quad & \mathscr{S}_c = 0.10, \\ \text{SL:} \quad & \mathscr{S}_c = 0.105, \end{aligned}$$

where H & T is from the experimental data of Holloway & Tavoularis (1992). There is a consistent trend for the SSG, 2DMFI and FLT models, when compared to the critical values for the rotating shear: the higher $(\Omega/S)_c$ for stabilization of the flow correspond to higher $\mathscr{S}_c$. The SL model has small but non-zero ϵ/Sk over the range $0.025 < \mathscr{S} < \mathscr{S}_c$.

Case 5. Two- and three-dimensional strains

The rapid-pressure model is used to compute three strain flows: plane strain and axisymmetric contraction and expansion. These flows are another test case as the rapid-pressure model has not used these flows to set the calibration coefficients. The results are compared to the DNS of Lee & Reynolds (1985). Because the simulations are conducted at low Reynolds number the anisotropies are expected to be somewhat higher than those of fully developed turbulence. However, the use of the physical experiments conducted at higher Reynolds number is also somewhat suspect as the initial conditions on ϵ/Sk, as has been pointed out by Speziale *et al.* (1991), are not known with certainty. The same test cases as those given in Speziale *et al.* (1991) are used. Our results are also compared to the SSG model as it appears to be the current model that gives the best results. The evolution of the kinetic energy for these flows is not presented; the results for the models are in very good agreement with the data and each other and do not definitively distinguish between the various models.

Figure 5(*a*) shows the evolution of the anisotropy for the plane strain, $S_{ij} = S^*(\delta_{i1}\,\delta_{j1} - \delta_{i2}\,\delta_{j2})$ starting from isotropic initial conditions. Figures 5(*b*) and 5(*c*) show the evolution of the anisotropy for the axisymmetric contraction and expansion. Here for the contraction $S_{ij} = S^*(\delta_{i1}\,\delta_{j1} - \frac{1}{2}\delta_{i2}\,\delta_{j2} - \frac{1}{2}\delta_{i3}\,\delta_{j3})$. For the expansion S is replaced with $-S$. Results for all the plane and axisymmetric strain flows capture the trends nicely.

10. General discussion

The constraints of geostrophy, realizability, joint-realizability, normalization and continuity have been used to create a variable-coefficient rapid-pressure representation that is frame indifferent in the two-componential limit, $\Omega_j u_j = 0$. The use of the MFI or the realizability-type constraints to obtain values of unknown coefficients in the models has been justifiably criticized on the grounds that one should not use extreme states to set unknown constants. It should be made clear that the present methodology does not use the limit states to fix the coefficients in the model: the present rapid-pressure covariance representation is not a constant-coefficient model and the extreme states have been invoked only to ensure that the variable coefficients in the rapid-pressure representation behave properly as the limit states are approached. Away from the extreme states the model coefficients vary in a way that reflects not the extreme states but the structural equilibrium state used to calibrate the model.

It should also be kept in mind that any rigorous interpretation of the physics of these

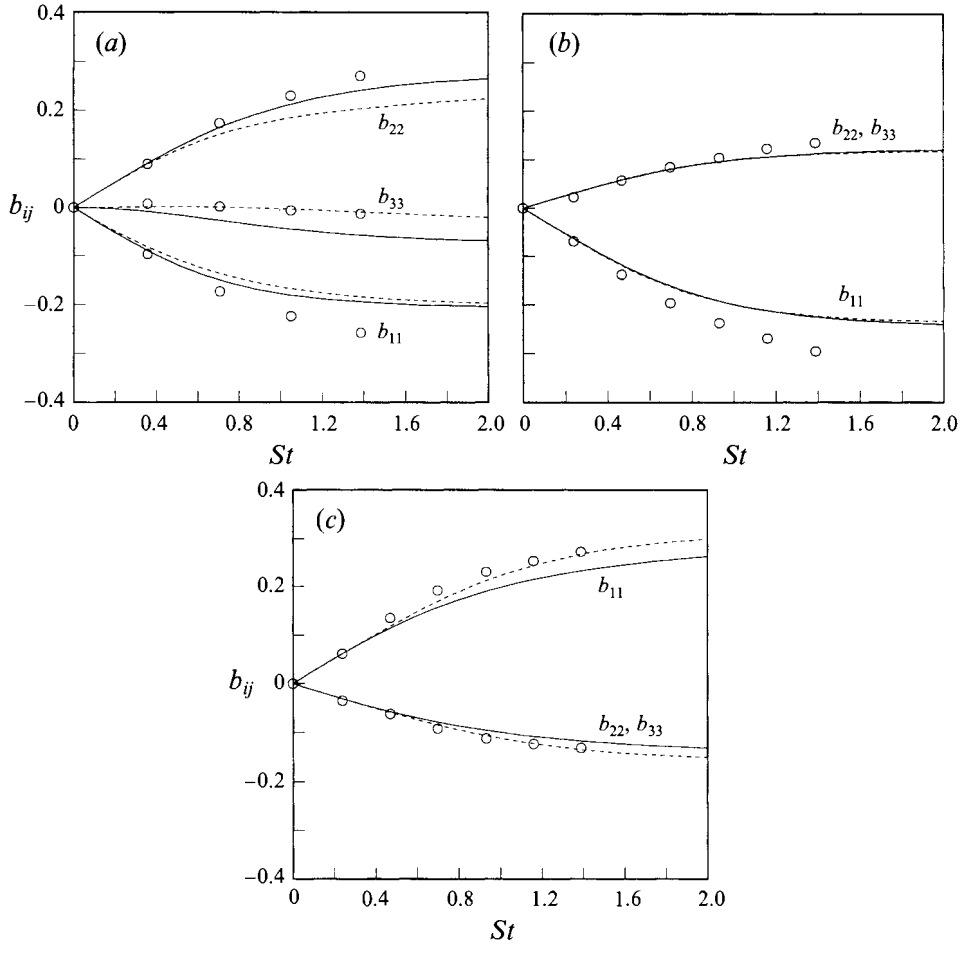

FIGURE 5. Time evolution for the anisotropy tensor: (*a*) plane strain for $\epsilon_0/Sk_0 = 2.0$, (*b*) the axisymmetric contraction for $\epsilon_0/Sk_0 = 0.179$, (*c*) the axisymmetric expansion for $\epsilon_0/Sk_0 = 2.45$. ——, The predictions of the 2DMFI model; – – –, the SL model; ○, the direct numerical simulations of Lee & Reynolds (1985).

realizability limits – requiring all the scales of the motion to be two-componential in an arbitrary plane – is inconsistent with the assumptions underlying the development of these turbulence modelling methods. However, from the point of view of a useful engineering approximation, the fact that the first decade, $\kappa\ell < 10$, following the arguments of §3, of the flow becomes two-componential means that the pertinent eigenvalue of the Reynolds stress becomes small. As the largest contribution to the rapid pressure is from the largest scales of the motion, the rapid-pressure covariance will begin to approach its realizable limit. This is not an unusual occurrence in flows of engineering interest. The anisotropy-invariance maps given in the works of Antonia, Djenidi & Spalart (1994*a*) and Antonia, Spalart & Mariani (1994*b*) using DNS of wall-bounded flows with and without suction indicate that the flow comes very close to the two-componential state: $F = 0$.

From a strictly practical point of view – computability – incorporating the realizability constraints into the models for unknown correlations has some very tangible and beneficial effects. During the convergence to a solution, from more or less arbitrary

initial conditions, the iteration will be plagued with negative normal stresses and correlation coefficients larger than one, either of which can destabilize and terminate the computation. When this occurs, the solution is clipped and the solution procedure restarted from the new clipped initial conditions. The frequency of this clipping and resetting procedure is substantially reduced (in simple flows even eliminated) when using realizable models. Part of the reluctance in accepting second-order modelling methods is that turbulence simulations of complex inhomogeneous flows with multi-dimensional mean flows which may have body forces, streamline curvature or rotational effects, are extremely difficult to compute; such difficulties are substantially reduced with realizable models.

How one obtains realizable turbulence is not an issue in problems with steady states, as long as the final state is realizable and the computation is not irrevocably destabilized during the computation. This, however, is not the case for problems that are unsteady. For time-varying flows for which second-order methods are still suitable realizability is a serious issue. Our experience with the Reynolds averaging procedure, in buoyantly driven elliptic flows with rotation, indicates that the averaging operation acts as a smoothing operation: the rapidly fluctuating instantaneous dynamics are subsumed by the averaging procedure leaving the slow-time large-scale parts of the flow, evolving on timescales commensurate with the integral timescale, to be captured by the computation. If the simulation is to reflect the physics of the time evolution of the flow, it must stay realizable. Clearly excessive realizability violations, requiring a clipping and resetting of the solution, which produces a solution that never evolves far from the transient associated with the most recent clipped initial condition, are not acceptable. In such flows, satisfying the realizability constraint has very important consequences for the validity of the time evolution of the flow.

The coefficients of the tensor polynomials used to present unknown quantities in a constitutive relation are, according to the theory, variable functions of the invariants of the independent tensors and, thus, depend on the state of the turbulence. The coefficients in 'realizable' turbulence models using some form of a realizability constraint are obtained by requiring that the rate of change of a positive semi-definite quantity be zero when some extreme state is reached. The coefficients so obtained are constants and are strictly valid only at the extreme state and yet are used to compute general flows that are nowhere near the extreme states. This is a fundamental limitation of all constant-coefficient models that use a limit state to set the model coefficients. In some models, one adds to the constant determined by the extreme state *ad hoc* corrections that depend on F, a quantity which parameterizes the departure from the realizable state. These corrections, which vanish as the limit state is approached, require some sort of numerical optimization involving several flows. This sketchily summarizes the methodology used in other 'realizable' turbulence models. In the quasi-linear SSG model the coefficients are, for the most part, constants that are also set by matching to a limit state. In the case of the SSG model the limit state is that of a structural equilibrium which is a much closer approximation to the turbulence expected to be seen in engineering problems. The constants in the SSG model may be viewed as the values of the non-constant coefficients near the equilibrium state.

In the present method the realizability principles are used to ensure that the coefficients in the constitutive relations, valid for all states of the mechanical turbulence, are consistent with realizability principles. Recall that the basic form of the rapid-pressure model comprises two parts: X^0_{ijkl} and FX^F_{ijkl}. X^0_{ijkl} satisfies simultaneously the five constraints – geostrophy, realizability, joint-realizability, normalization and continuity, while FX^F_{ijkl}, also obtained analytically, satisfies the

substantially less extreme joint-realizability as well as the homogeneous form of the normalization and continuity constraints. Thus, although the model coefficients are consistent with an extreme state, they are not constants fixed to their values at the extreme state. An extreme state of the flow has only been used to ensure that the variable coefficients have the proper behaviour in this limit – not to fix or calibrate the coefficients. The coefficients in the X^0_{ijkl} part of the model along with the additional FX^F_{ijkl} terms are, for the mechanical turbulence, fully general.

It is to this basic model, valid for all states of turbulence, that one adds the FX^∞_{ijkl} term that is necessary to attract the solution to its fixed points from arbitrary initial conditions. The requirement of asymptotic consistency with an equilibrium state, first used by Speziale *et al.* (1990*b*), is the single most empirically consistent physical requirement one can impose. Second-order closure methodology is built around the assumption that there is, to a suitable approximation, for the class of flows to which second-order methods are appropriate, an equilibrium state and in the absence of disturbing forces the flow relaxes to that state on a timescale similar to the eddy turnover time. There is very little evidence pointing to the fact that a unique equilibrium state exists. Such an equilibrium will be weakly dependent on initial conditions. The issue, however, is whether such an assumption is a useful approximation for the flows that these Reynolds stress models can be used to calculate. The weakness of the dependence suggests such is the case. It is this phenomenological behaviour that is built into the model by requiring the fixed points of the modelled equations to be consistent with those obtained from experiment. The assumption that allows the parameterization of the two-point correlation as a local function of the anisotropy tensor, $X_{ijkl} = X_{ijkl}\,(b_{ij})$, is also such an equilibrium assumption.

The penalty paid for these additional features associated with the satisfaction of the mathematical constraints is a more complex model. It should, however, be pointed out that the present 2DMFI model has the same tensor bases as the FLT model and is therefore no more complex except for the expressions for the non-constant coefficients. Moreover, the penalty is slight in the light of the reduction of the computational difficulties found during the calculation of quasi-steady time-evolving flows with this representation for the rapid pressure. The model, along with several others, has been used to compute inhomogeneous buoyancy-driven rotating flows that occur in the Czochralski crystal growth melt in which the Reynolds stress are three-dimensional (Ristorcelli & Lumley 1991*a*, 1993; Ristorcelli 1991). In computing these time-varying flows it was found that the present 2DMFI model produced virtually no realizability violations during the course of the flow evolution. For a quasi-steady flow this is a crucial point: every time realizability is violated the solution is reset and the solution never evolves past the transients associated with reseting the initial conditions. Such a computation cannot be expected to reflect an ensemble average of the original system.

11. Limitations, shortcomings and suggestions for future work

In the effort to produce a representation for the rapid-pressure correlation valid for the class of flows to which second-order modelling is suitable, some shortcomings in the data on homogeneous 'building block' flows have become apparent. Though homogeneous shear seems reasonably well-documented it is not clear whether the asymptotic states have been reached in some of the experiments. Moreover, the discrepancy between the high values of b^∞_{11} obtained in the DNS versus those seen in the laboratory data has not been explained. Additional work expanding on the notion of two classes of flows as suggested in Tavoularis & Karnik (1989) might be considered.

For homogeneous shear with rotation, a very basic flow, there seem to be no substantial data – LES, DNS or experimental – definitively describing its stationary states. At the very least, an assessment of the bifurcation diagram $(\epsilon/Sk)_\infty$ versus $(\Omega/S)_\infty$ predicted by the linear theory would be useful. Also the equilibrium values $(\mathscr{P}/\epsilon)_\infty$ would be useful for further developments regarding the dissipation equation's dependence on rotation. This may remedy the under-prediction of the kinetic energy growth rates as a function of Ω/S for all the models. The present class of dissipation equations predicts an asymptotic state in which $(\mathscr{P}/\epsilon)_\infty$ is a model-dependent constant, which for all rotation rates has the same value as in asymptotic shear. Had the stationary values of the anisotropy tensor and $(\mathscr{P}/\epsilon)_\infty$ and $(\epsilon/Sk)_\infty$ been available, application of the present methodology would have produced a set of modelled evolution equations whose fixed points matched the fixed points of rotating shear, independent of the deficiencies in the dissipation equation. The present calibration has used only equilibrium data and hence is independent of the model form of the dissipation equation. This then leads naturally to the fixed-point behaviour of these classes of turbulence models; some useful thoughts on this issue are given in Speziale *et al.* (1991).

The geostrophic constraint results from the fact that a wide class of horizontally divergence-free fields, $\Omega_j u_{3,j} = 0$, are frame indifferent. This implies very little about either the vector components of the velocity field or its dependence on the spatial coordinates: its componentiality or its dimensionality. The simultaneous satisfaction of the geostrophic and realizability constraints means that the present representation cannot treat a general three-componential MFI turbulence, i.e. one in which $\Omega_j u_j \neq 0$ but $\Omega_j u_{i,j} = 0$. This is a direct consequence of the fact that any parameterization of the unknown quantities in terms of only the Reynolds stresses cannot account for the anisotropy of the two-point fields. In problems of engineering interest, the flow field is typically bounded and has no-flux (or only steady-flux) boundary conditions. In such situations the materially frame-indifferent turbulence field will also be the $\Omega_j u_j = 0$ field. It is this vision of a flow of engineering interest that forms the choice to satisfy simultaneously the geostrophic and realizable constraints in spite of the loss of generality, which does not appear to be possible anyway in the context of these types of single-point Reynolds stress closures.

In §6 the nature of the singular representation of the volume integral of the two-point velocity correlation brought to our attention by Reynolds (1994) was discussed. As pointed out by Reynolds (1994), the expression for the rapid-pressure covariance at the one-dimensional limit is singular and depends on the relative rates at which the two eigenvalues are lost. Reynolds (1994) has shown that $X_{1133} = 0$ and $X_{1122} = 1$ if one approaches the one-dimensional limit with one eigenvalue already zero; while $X_{1122} = X_{1133} = \frac{1}{2}$ if the limit is approached when both eigenvalues are lost at the same rate. The relevance of this singularity in the context of the model has been discussed above; Reynolds (1994) gives a discussion with respect to the implied dimensionality of the instantaneous velocity field. The fundamental issue here is about the two-point correlation of the field. When X_{ijkl} is parameterized in terms of the one-point Reynolds stress it is found that when $\langle u_3 u_3 \rangle$ vanishes X_{1133} also vanishes. Such models cannot distinguish a flow field that has lost an eigenvalue $\langle u_3 u_3 \rangle$ from a flow field that is perfectly coherent in the x_3 direction. This stems from the fact that the parameterization of the energy spectrum solely in terms of the anisotropy tensor is incomplete, as has been seen in rapidly rotating isotropic flows in which there is a very strong anisotropy of the coherence. This is a very interesting point theoretically and clearly delineates the class of flows that this type of model cannot handle. This limitation is an area of

research that Reynolds has been following; Reynolds & Kassinos (1994) contains recent developments.

The present rapid-pressure model is expected to distinguish itself in complex three-dimensional flows. For the planar flows for which test cases exist the model outperforms the nonlinear models using realizability-type constraints. It is only moderately better than the topologically generic form of the SSG model suitable for simple planar flows. It is unfortunate that there exist no suitable DNS or LES of flows in which the presence of a body force causes the larger scales of the motion to become quasi-two-componential. Such a test case would help further establish the utility of incorporating some of the more complex physics into the structure of the model as well as, perhaps, pointing out the potential deficiencies of models developed using simple planar mean flows.

12. Summary and conclusions

A representation of the rapid-pressure–strain correlation with a minimum of *ad hoc* constants has been devised. The rapid-pressure model produces the proper behaviour in five different limits:

(i) the materially frame-indifferent limit in which the eigenvalues of the Reynolds stress tensor, $\langle u_i u_j \rangle$, and $\langle \theta\theta \rangle \langle u_i u_j \rangle - \langle \theta u_i \rangle \langle \theta u_j \rangle$ aligned with the axis of rotation, vanish;

(ii) the realizable limit in which the eigenvalue of the Reynolds stress tensor aligned in an arbitrary direction vanishes;

(iii) the joint-realizable limit in which an arbitrary eigenvalue of

$$\langle \theta\theta \rangle \langle u_i u_j \rangle - \langle \theta u_i \rangle \langle \theta u_j \rangle$$

vanishes;

(iv) the isotropic limit in which the anisotropy tensor, $b_{ij} = 0$, vanishes;

(v) the asymptotic structural equilibrium limit in which $(\mathrm{D}/\mathrm{D}t)\, b_{ij} = 0$. The general form of the model is

$$X_{ijkl} = X^0_{ijkl} + FX^F_{ijkl} + FX^\infty_{ijkl},$$

where the X_{ijkl} are polynomials in the anisotropy tensor. X^0_{ijkl} satisfies the following five constraints: the limit states of (i) geostrophy, (ii) realizability, (iii), joint-realizability, and the integral constraints of (iv) continuity and (v) normalization. X^F_{ijkl} satisfies the three constraints of joint-realizability, continuity and normalization. Both X^0_{ijkl} and FX^F_{ijkl} are obtained analytically: the represent the simplest analytical expressions that are capable of satisfying all the mathematical constraints. The first four limit states are used to ensure that the variable model coefficients behave properly as each of the limit states is approached; they are not used to calibrate or set the coefficients to some constant value valid only at a limit state.

X^∞_{ijkl}, on the other hand, is obtained by requiring asymptotic consistency with a structural equilibrium state and does involve setting the coefficients to a particular constant value corresponding to a specific flow situation. The experimentally determined stationary values of the anisotropy tensor, b^∞_{ij}, and $(\mathscr{P}/\epsilon)_\infty$ and $(\epsilon/Sk)_\infty$ have been used to ensure that the fixed points of the modelled equations match the experimentally determined fixed points. This process, in as much as it has been carried out for the homogeneous shear, should produce a useful model for three-dimensional mean flows in which the mean shear is an important production mechanism. It should be noted that this calibration procedure is done for a particular model for the return pressure covariance. The representation can be recalibrated for a different class of flows or a different return model.

A few novel points, regarding the rapid-pressure covariance representation merit special mention:

(i) The present representation of the rapid-pressure covariance has variable coefficients. All the coefficients in the basic portion of the model are obtained from first principles: they are functions of the state of the turbulence and are valid for all states of mechanical turbulence. The coefficients are not constants fixed to their values at extreme or equilibrium states – the extreme states have been used only to ensure that the variable coefficients in the rapid-pressure representation behave properly as these limit states are approached.

(ii) Away from the extreme states the model coefficients vary in a way that does not reflect the extreme states but the structural equilibrium state used to calibrate the model. The present form of the model is consistent with the equilibrium homogeneous shear. This ensures, with the removal of disturbing forces, that the flow relaxes to the fixed points of the homogeneous shear.

(iii) The rapid-pressure covariance representation is at present the only variable-coefficient model that is consistent with the fact that materially frame-indifferent flows are horizontally divergence free. In bounded flows of geophysical or engineering interest a vanishing horizontal divergence, $\Omega_j u_{i,j} \delta_{i3} \to 0$, is typically accompanied by $\Omega_j u_j \to 0$. This MFI requirement for the representation has been satisfied by ensuring that the geostrophic constraint is satisfied as $\Omega_j u_j$ vanishes.

The frame-indifference requirement was first realized in the context of flows dependent on only two independent variables (Speziale 1981, 1985, 1989). There are, however, several classes of MFI flows that do not fall in the 2DMFI category. It has been shown that when the velocity is horizontally divergence free the vertical vorticity equation, which is the evolution equation for the streamfunction, is MFI. MFI of the whole field is then determined by the nature of the equation for the vertical velocity. If (i) $w = 0$ or (ii) the pressure is independent of the axial coordinate or (iii) determined by a hydrostatic balance with the temperature then the flow will be MFI. Such flows in which MFI is a consideration occur in small-aspect-ratio situations or in flows in which a strong stable stratification or magnetic fields acts to 'two-componentialize' the flow. In bounded rotating flows the satisfaction of the geostrophic constraint ensures consistency with the Taylor–Proudman theorem: the modelled equations are frame indifferent when the vanishing of $\Omega_j u_j$ is the result of Coriolis forces.

There is some interesting physics underlying this mathematical requirement. In general an MFI flow is one that is non-divergent in a plane defined by the axis of rotation. Thus an MFI flow is one in which the stretching of vorticity along the axis of rotation is, for whatever reason, vanishingly small.

This frame invariance for specific classes of horizontally divergence-free fields is the most notable feature of the model and is expected to be important for the computation of engineering and geophysical flows in which dynamical or kinematical agencies leading to such a condition are important. These flows might include: (i) turbulence in which a strong stable stratification suppresses the vertical component of the velocity field; (ii) turbulence affected by magnetic fields; (iii) turbulence influenced by centrifugal forces associated with streamline curvature such as those that occur in turbomachinery, swirling combustion, tornadoes, or in the growth of crystals; (iv) turbulence influenced by Coriolis forces in which the largest scales of the flow are nominally two-componential, obeying shallow-water-type equations such as those occurring in large-scale geophysical flows in which a geostrophic limit is attained outside the boundary layers; (v) turbulence near a free surface at which one of the components of the fluctuating velocity is suppressed; (vi) the environmentally

important shallow-water flows such as those associated with waste heat exchange, near-shore pollution dispersal, and mixing associated with thermal and salinity inflows. However, until suitable data bases, DNS or LES, of these complex flows with body forces become available, the full potential of a rapid-pressure model built from first principles in three-dimensional flows cannot be verified. The present model does however reproduce the experimental data at least as well as the currently available models for a wide class of planar flows for which experimental data is available.

J. R. R. acknowledges several fruitful conversations with Professor C. G. Speziale. It is also a pleasure to thank Professor W. C. Reynolds who, abandoning his referee's anonymity, cheerfully but unrelentingly impelled us to a deeper consideration of horizontally divergence-free issues, until we finally got it right. Thanks also are due to Dr T. B. Gatski whose calculations of the homogeneous strain test cases helped complete the paper. The basic aspects of the work were completed at Cornell University during the PhD studies of J. R. R. During that time support was primarily from the US National Science Foundation Grant No. MSM-8611164 for Czochralski crystal growth. Support also came from the US Office of Naval Research under the programs Physical Oceanography (Code 422PO), Power (Code 473). Subsequent developments of the model have been carried out at ICASE.

Appendix A. A synopsis of the final rapid-pressure correlation representation

For convenience and clarity the final form of the model is summarized here. The general final form of the model is

$$\begin{aligned}\Pi^r_{ij}/2q^2 = {} & [C_3 - 2\mathrm{II}C_3'' + 3\mathrm{III}C_3''']S_{ij} \\ & + C_4[b_{ip}S_{pj} + b_{jp}S_{pi} - \tfrac{2}{3}\langle bS\rangle \delta_{ij}] + C_4'''\langle bS\rangle [b^2_{ij} + 2\mathrm{II}/3\delta_{ij}] \\ & + C_5[b_{ip}W_{pj} + b_{jp}W_{pi}] + [C_6\langle bS\rangle + C_4'''\langle b^2S\rangle]b_{ij} \\ & + C_7[b^2_{ip}S_{pj} + b^2_{jp}S_{pi} - \tfrac{2}{3}\langle b^2S\rangle \delta_{ij}] \\ & + C_8[b^2_{ip}W_{pj} + b^2_{jp}W_{pi}] + C_9[b_{ip}W_{qp}b^2_{qj} + b_{jp}W_{qp}b^2_{qi}].\end{aligned}$$

For flows in rotating coordinate systems, W_{ij} appearing in Π^r_{ij} must be replaced by the total rotation tensor $W_{ij} + \epsilon_{jik}\Omega_k$. The coefficients C_i are given by a sum of the basic model coefficients, B_i, which come from first principles, and the calibration coefficients A^c_i. The basic model coefficients are related to the coefficients A_i in the fourth-order tensor polynomial expression by

$$\begin{aligned}B_3 &= 2(A_1 + A_2) = \tfrac{2}{27}[41 + 42\mathrm{II} - 0.1F(221 + 420\mathrm{II})]/\mathrm{II}_d, \\ B_3'' &= A_9 + A_{10} = -\tfrac{14}{3}(1 + 3\mathrm{II})/\mathrm{II}_d + 0.6F/(1 + 3\mathrm{II}), \\ B_3''' &= -\tfrac{1}{3}(A_{11} + A_{12} + 2A_{13}) = (55 + 84\mathrm{II})/3\mathrm{II}_d, \\ B_4 &= A_3 + A_4 + 2A_5 = 3/\mathrm{II}_d - 0.9F/(1 + 3\mathrm{II}), \\ B_4''' &= A_{11} + A_{12} + 4A_{13} = -9/\mathrm{II}_d, \\ B_5 &= A_3 - A_4 = -\tfrac{1}{30}(10 + 21F)/(1 + 3\mathrm{II}), \\ B_6 &= 2A_9 + 4A_{10} = -18\mathrm{II}/\mathrm{II}_d + 3F/(1 + 3\mathrm{II}), \\ B_7 &= A_6 + A_7 + 2A_8 - 2A_9 - 2A_{10} = -9/\mathrm{II}_d - 1.8F/(1 + 3\mathrm{II}), \\ B_8 &= A_6 - A_7 = \tfrac{1}{5}(3F - 5)/(1 + 3\mathrm{II}), \\ B_9 &= A_{11} - A_{12} = -3/(1 + 3\mathrm{II}).\end{aligned}$$

The A_i are given in Appendix C. The C_i, which reflect the application of the additional constraint, asymptotic consistency with an equilibrium state, are obtained from the B_i using $C_i = B_i + FA_i^c$. They are given by

$$
\begin{aligned}
C_3 &= B_3 - 2F(10A_8^c + 3A_9^c + A_{10}^c)\,\mathrm{II}/5 - F(A_{11}^c + A_{12}^c + 14A_{13}^c))\,\mathrm{III}/5,\\
C_3'' &= B_3'' + F(A_9^c + A_{10}^c),\\
C_3''' &= B_3''' - \tfrac{1}{3}F(A_{11}^c + A_{12}^c + 2A_{13}^c),\\
C_4 &= B_4 + F(-3A_5^c + \mathrm{II}(A_{11}^c + A_{12}^c + 4A_{13}^c)),\\
C_4''' &= B_4''' + F(A_{11}^c + A_{12}^c + 4A_{13}^c),\\
C_5 &= B_5 + F(-\tfrac{7}{3}A_5^c + \tfrac{1}{3}\mathrm{II}(-A_{11}^c + 3A_{12}^c + 4A_{13}^c)),\\
C_6 &= B_6 + F(2A_9^c + 4A_{10}^c),\\
C_7 &= B_7 - 3F(A_8^c + A_9^c + A_{10}^c),\\
C_8 &= B_8 - \tfrac{1}{3}F(7A_8^c + 3A_8^c + 3A_9^c - A_{10}^c),\\
C_9 &= B_9 + F(A_{11}^c - A_{12}^c),
\end{aligned}
$$

where the A_i^c are expressed in terms of the seven free parameters $A_i^c\{i = 5, 8\text{–}13\}$. Without further specifying the calibration coefficients, A_i^c, the above rapid-pressure model is general, suitable for the flows for which second-order modelling is suitable. Calibration to a particular archetypal flow, by matching the fixed points of the modelled evolution equations with experimentally determined fixed points, will result in a model suitable for diverse flows within that class of flows. For a flow in which the dominant production mechanism is associated with the mean shear, homogeneous shear is used to set the model coefficients. Asymptotic consistency with homogeneous equilibrium shear and a linear model for the return coefficient produce the following values for the calibration coefficients:

$$
\begin{aligned}
A_5^c &= -0.29 + 0.06(A_{10}^c - A_8^c),\\
A_{11}^c &= -3.6 + 5A_{10}^c - 2A_{13}^c - 12.7A_8^c - 3.8A_9^c,\\
A_{12}^c &= -24.5 - 44.8A_{10}^c - 2A_{13}^c + 28.7A_8^c - 8.65A_9^c,
\end{aligned}
$$

where $A_8^c = 0.6$, $A_9^c = -0.6$, $A_{10}^c = -0.15$, $A_{13}^c = 0$. The calibration coefficients reflect the asymptotic value of the coefficients in the return-to-isotropy model used. The usual canonical form $-\mathrm{C}_1\,\epsilon b_{ij} + C_2\,\epsilon[b_{ij}^2 + 2\mathrm{II}/3\delta_{ij}]$ with $C_2 = 0$ and $C_1 = 2 - 31\mathrm{II}F^{1/2}$ is used.

The homogeneous forms of the continuity and normalization conditions have been used to produce relations between the free parameters. They are

$$
\begin{aligned}
&A_1^c + 4A_2^c - 2A_8^c\,\mathrm{II} + \mathrm{III}(A_{11}^c + A_{12}^c + 2A_{13}^c) = 0,\\
&A_3^c + A_4^c + 5A_5^c - \mathrm{II}(A_{11}^c + A_{12}^c + 4A_{13}^c) = 0,\\
&A_6^c + A_7^c + 5A_8^c + A_9^c + A_{10}^c = 0,
\end{aligned}
$$

$$
\begin{aligned}
&3A_1^c + 2A_2^c - 2A_6^c\,\mathrm{II} + 4A_{13}^c\,\mathrm{III} = 0,\\
&3A_4^c + 4A_5^c - 2\mathrm{II}(A_{11}^c + 2A_{13}^c) = 0,\\
&3A_7^c + 4A_8^c + 2A_{10}^c = 0.
\end{aligned}
$$

The fact that the A_i^c must satisfy these equations has been used to express six of the $A_i^c\{i = 1\text{–}4, 6, 7\}$ in terms of the seven $A_i^c\{i = 5, 8\text{–}13\}$ in the expressions for the $C_i = B_i + FA_i^c$.

Appendix B. The calibration coefficients in the rapid-pressure representation

The calibration process is described in more detail in this Appendix. The model has been calibrated to match the fixed points of homogeneous shear. The following equations describe the evolution of the anisotropy tensor:

$$(\mathrm{D}/\mathrm{D}t)/\, b_{ij} = -2\epsilon_{ikp}\, b_{pj}\, \Omega_k - 2\epsilon_{jkp}\, b_{pi}\, \Omega_k - [b_{ip}\, U_{j,p} + b_{jp}\, U_{i,p} - \tfrac{2}{3}\delta_{ij}\langle bS\rangle] \\ -\tfrac{2}{3}S_{ij} + 2b_{ij}\langle bS\rangle + \Pi^r_{ij}/q^2 - (C_1 - 2)\, b_{ij}\, \epsilon/q^2 + C_2[b^2_{ij} + 2\mathrm{II}/3\delta_{ij}]\, \epsilon/q^2.$$

For the planar flow case with axial mean flow and mean shear, $U_{1,2}$, the algebraic equations for the fixed points, setting $(\mathrm{D}/\mathrm{D}t)\, b_{ij} = 0$, become

$$(b_{11} + \tfrac{1}{3})(2 + 4b_{12}\, Sk/\epsilon) - 4b_{12}\, Sk/\epsilon + (Sk/\epsilon)\, \Pi^r_{11}/(Sk) - C_1\, b_{11} - \tfrac{2}{3} \\ + C_2(b_{11}\, b_{11} + b_{12}\, b_{12} + \tfrac{2}{3}\mathrm{II}) - 8(\Omega/S)\, (Sk/\epsilon)\, b_{12} = 0,$$

$$b_{12}(2 + 4b_{12}\, Sk/\epsilon) - 2(b_{22} + \tfrac{1}{3})\, Sk/\epsilon + (Sk/\epsilon)\, \Pi^r_{12}/(Sk) - C_1\, b_{12} \\ + C_2\, b_{12}(b_{11} + b_{22}) + 4(\Omega/S)\, (Sk/\epsilon)\, (b_{11} - b_{22}) = 0,$$

$$(b_{22} + \tfrac{1}{3})(2 + 4b_{12}\, Sk/\epsilon) + (Sk/\epsilon)\, \Pi^r_{22}/(Sk) - C_1\, b_{22} - \tfrac{2}{3} \\ + C_2(b_{22}\, b_{22} + b_{12}\, b_{12} + \tfrac{2}{3}\mathrm{II}) + 8(\Omega/S)\, (Sk/\epsilon)\, b_{12} = 0,$$

$$(b_{33} + \tfrac{1}{3})(2 + 4b_{12}\, Sk/\epsilon) + (Sk/\epsilon)\, \Pi^r_{33}/(Sk) - C_1\, b_{33} - \tfrac{2}{3} + C_2(b_{33}\, b_{33} + \tfrac{2}{3}\mathrm{II}) = 0.$$

The last equation for b_{33} is not linearly independent as $b_{jj} = 0$. The following fixed point values are taken to be representative: $b^\infty_{11} = 0.203$, $b^\infty_{12} = -0.156$, $b^\infty_{22} = -0.143$, $b^\infty_{33} = -0.06$, $(Sk/\epsilon)_\infty = 5.54$, $(\mathscr{P}/\epsilon)_\infty = 1.73$. They represent an average of numerical and experimental data as given in the text. Inserting the data into the algebraic equations above produces the following values of the invariants for the anisotropy tensor: $\mathrm{II}_\infty = -0.0587$, $\mathrm{III}_\infty = 0.0032$, $F_\infty = 0.5736$. The solution of the algebraic equations describing the stationary state of homogeneous shear produces the following values for the calibration coefficients:

$$A^c_5 = -0.3388 + 0.06(A^c_8 + A^c_{10}) + 0.015C^\infty_1 - 0.008C^\infty_2,$$

$$A^c_{11} = -14.35 - 2A^c_{13} - 12.68A^c_8 + 3.80A^c_9 - 5.072A^c_{10} + 3.157C^\infty_1 + 0.5898C^\infty_2,$$

$$A^c_{12} = -16.87 - 2A^c_{13} + 28.7A^c_8 - 8.05A^c_9 - 44.81A^c_{10} - 12.17C^\infty_1 - 0.291C^\infty_2.$$

The model has been left as general as possible – allowing for any return term of the canonical form $-C_1\, \epsilon b_{ij} + C_2[b^2_{ij} + 2\mathrm{II}/3\delta_{ij}]$, where the C_i are not necessarily constants but have achieved their asymptotic values $C_i = C^\infty_i$. Choosing a linear Rotta-type return term setting the nonlinear return coefficient to zero, $C_2 = 0$, produces

$$A^c_5 = -0.29 + 0.06(A^c_{10} - A^c_8),$$

$$A^c_{11} = -3.6 + 5A^c_{10} - 2A^c_{13} - 12.7A^c_8 - 3.8A^c_9,$$

$$A^c_{12} = -24.5 - 44.8A^c_{10} - 2A^c_{13} + 28.7A^c_8 - 8.65A^c_9,$$

where the following values of the free parameters have been chosen: $A^c_8 = 0.6$, $A^c_9 = -0.6$, $A^c_{10} = -0.15$, $A^c_{13} = 0$. Note that this calibration is independent of the dissipation equation but not independent of the return pressure model. These indicated calibration coefficients are appropriate for the class of flows in which the mean shear is the predominant production mechanism.

The component form of the rapid pressure used in the equations for the stationary state is

$$
\begin{aligned}
\Pi_{11}^{r}/2q^2S^* &= C_4 b_{12}/3 + C_4'''(b_{11}b_{11}+b_{12}b_{12}+2\mathrm{II}/3)b_{12} + C_5 b_{12}(-W^*/S^*)\\
&\quad + [C_6 + C_4'''(b_{11}+b_{22})]b_{11}b_{12} + C_7(b_{11}+b_{22})b_{12}/3\\
&\quad + C_8(b_{11}+b_{22})b_{12}(-W^*/S^*) + C_9(W^*/S^*)b_{12}(b_{12}b_{12}-b_{11}b_{22}),\\
\Pi_{22}^{r}/2q^2S^* &= C_4 b_{12}/3 + C_4'''(b_{22}b_{22}+b_{12}b_{12}+2\mathrm{II}/3)b_{12} + C_5 b_{12}(W^*/S^*)\\
&\quad + [C_6 + C_4'''(b_{11}+b_{22})]b_{22}b_{12} + C_7(b_{11}+b_{22})b_{12}/3\\
&\quad C_8(b_{11}+b_{22})b_{12}(W^*/S^*) + C_9(-W^*/S^*)b_{12}(b_{12}b_{12}-b_{11}b_{22}),\\
\Pi_{12}^{r}/2q^2S^* &= \tfrac{1}{2}[C_3 - 2\mathrm{II}C_3'' + 3\mathrm{III}C_3'''] + \tfrac{1}{2}C_4(b_{11}+b_{22}) + C_4'''(b_{11}+b_{22})b_{12}b_{12}\\
&\quad + C_5(b_{11}-b_{22})(W^*/2S^*) + [C_6 + C_4'''(b_{11}+b_{22})]b_{12}b_{12}\\
&\quad + \tfrac{1}{2}C_7(b_{11}b_{11}+2b_{12}b_{12}+b_{22}b_{22})\\
&\quad + C_8(b_{11}b_{11}-b_{22}b_{22})(W^*/2S^*) + C_9(b_{11}b_{22}-b_{12}b_{12})(b_{11}-b_{22})\\
&\quad \times (W^*/2S^*),\\
\Pi_{33}^{r}/2q^2S^* &= -\tfrac{2}{3}C_4 b_{12} + C_4'''(b_{33}b_{33}+2\mathrm{II}/3)b_{12} + (C_6 + C_4'''(b_{11}+b_{22}))b_{12}b_{33}\\
&\quad -\tfrac{2}{3}C_7 b_{12}(b_{11}+b_{22}).
\end{aligned}
$$

Appendix C. The Cayley–Hamilton theorem generalization

Reference has been made to a generalized Cayley–Hamilton theorem (Rivlin 1955) relating different powers of products of matrices.

$$
\begin{aligned}
&\boldsymbol{ABC}+\boldsymbol{ACB}+\boldsymbol{BCA}+\boldsymbol{BAC}+\boldsymbol{CAB}+\boldsymbol{CBA}\\
&\quad = \boldsymbol{A}(\langle BC\rangle - \langle B\rangle\langle C\rangle) + \boldsymbol{B}(\langle CA\rangle - \langle C\rangle\langle A\rangle) + \boldsymbol{C}(\langle AB\rangle - \langle A\rangle\langle B\rangle)\\
&\qquad + (\boldsymbol{BC}+\boldsymbol{CB})\langle A\rangle + (\boldsymbol{CA}+\boldsymbol{AC})\langle B\rangle + (\boldsymbol{AB}+\boldsymbol{BA})\langle C\rangle\\
&\qquad + \mathbf{1}[\langle A\rangle\langle B\rangle\langle C\rangle - \langle A\rangle\langle BC\rangle - \langle B\rangle\langle AC\rangle - \langle C\rangle\langle AB\rangle\\
&\qquad + \langle ABC\rangle + \langle CBA\rangle].
\end{aligned}
$$

The Cayley–Hamilton generalization is easily derivable from the Cayley–Hamilton theorem applied to sums and differences of matrices $\boldsymbol{A}$, $\boldsymbol{B}$, $\boldsymbol{C}$. The theorem is useful in eliminating redundant tensor bases in tensor representation theorems. Here $\langle\ \rangle$ is used to indicate the trace. The Cayley–Hamilton theorem for the anisotropy tensor is $\boldsymbol{b}^3 = \frac{1}{3}\langle b^3\rangle\mathbf{1} + \frac{1}{2}\langle b^2\rangle\boldsymbol{b}$. The theorem can also be used to express

$$
\begin{aligned}
\boldsymbol{bSb} &= -[\boldsymbol{b}^2\boldsymbol{S}+\boldsymbol{Sb}^2] + \langle bS\rangle\boldsymbol{b} + \tfrac{1}{2}\langle b^2\rangle\boldsymbol{S} + \langle b^2S\rangle\mathbf{1},\\
\boldsymbol{bSb}^2+\boldsymbol{b}^2\boldsymbol{Sb} &= -\tfrac{1}{3}\langle b^3\rangle\boldsymbol{S} + \langle b^2S\rangle\boldsymbol{b} + \langle bS\rangle\boldsymbol{b}^2.
\end{aligned}
$$

Appendix D. The rapid-pressure models

The detailed forms of the pressure–strain models referred to in this paper are as follows:

The Launder, Reece & Rodi model (LRR)

$$\Pi_{ij} = -2C_1\,\epsilon b_{ij} + \tfrac{4}{5}KS_{ij} + C_2K(b_{ik}S_{jk} + b_{jk}S_{ik} - \tfrac{2}{3}b_{kl}S_{kl}\delta_{ij}) + C_3K(b_{ik}W_{jk} + b_{jk}W_{ik}),$$

where

$$C_1 = 1.5, \quad C_2 = 1.75, \quad C_3 = 1.31.$$

The Shih & Lumley model (SL)

$$\begin{aligned}\Pi_{ij} = &-\beta\epsilon b_{ij} + \tfrac{4}{5}KS_{ij} + 12\alpha_5 K(b_{ik}S_{jk} + b_{jk}S_{ik} - \tfrac{2}{3}b_{kl}S_{kl}\delta_{ij})\\ &+ \tfrac{4}{5}(2-7\alpha_5)K(b_{ik}W_{jk} + b_{jk}W_{ik})\\ &+ \tfrac{4}{5}K(b_{il}b_{lm}S_{jm} + b_{jl}b_{lm}S_{im} - 2b_{ik}S_{kl}b_{lj} - 3b_{kl}S_{kl}b_{ij})\\ &+ \tfrac{4}{5}K(b_{il}b_{lm}W_{jm} + b_{jl}b_{lm}W_{im}),\end{aligned}$$

where

$$\beta = 2 + \frac{\Phi}{9}\exp(-7.77/Re_t^{1/2})\{72/RE_t^{1/2} + 80.1\ln[1 + 62.4(-\mathrm{II} + 2.3\mathrm{III})]\}$$

$$F = 1 + 9\mathrm{II} + 27\mathrm{III}, \quad \mathrm{II} = -\tfrac{1}{2}b_{ij}b_{ij}, \quad \mathrm{III} = \tfrac{1}{3}b_{ij}b_{jk}b_{ki}$$

$$Re_t = Re_t = \frac{4}{9}\frac{K^2}{\nu\epsilon}, \quad \alpha_5 = \frac{1}{10}\left(1 + \frac{4}{5}F^{1/2}\right).$$

The Fu, Launder & Tselepidakis model (FLT)

$$\begin{aligned}\Pi_{ij} = &\beta_1\,\epsilon b_{ij} + \beta_2\,\epsilon(b_{ik}b_{kj} - \tfrac{1}{3}b_{kl}b_{kl}\delta_{ij}) + \tfrac{4}{5}KS_{ij} + 1.2K(b_{ik}S_{jk} + b_{jk}S_{ik} - \tfrac{2}{3}b_{kl}S_{kl}\delta_{ij})\\ &+ \tfrac{26}{15}K(b_{ik}W_{jk} + b_{jk}W_{ik}) + \tfrac{4}{5}K(b_{ik}b_{kl}S_{jl} + b_{jk}b_{kl}S_{il} - 2b_{ik}S_{kl}b_{lj} - 3b_{kl}S_{kl}b_{ij})\\ &+ \tfrac{4}{5}K(b_{ik}b_{kl}W_{jl} + b_{jk}b_{kl}W_{il}) - \tfrac{14}{5}K[8\mathrm{II}(b_{ik}W_{jk} + b_{jk}W_{ik})\\ &+ 12(b_{ik}b_{kl}W_{lm}b_{mj} + b_{jk}b_{kl}W_{lm}b_{mi})],\end{aligned}$$

where

$$\beta_1 = 120\mathrm{II}F^{1/2} + 2F^{1/2} - 2, \quad \beta_2 = 144\mathrm{II}F^{1/2}$$

The Speziale, Sarkar & Gatski model (SSG)

$$\begin{aligned}\Pi_{ij} = &-(2C_1\,\epsilon + C_1^*\mathscr{P})b_{ij} + C_2\,\epsilon(b_{ik}b_{kj} - \tfrac{1}{3}b_{kl}b_{kl}\delta_{ij}) + (C_3 - C_3^*\,\mathrm{II}_b^{1/2})KS_{ij}\\ &+ C_4K(b_{ik}S_{jk} + b_{jk}S_{ik} - \tfrac{2}{3}b_{kl}S_{kl}\delta_{ij}) + C_5K(b_{ik}W_{jk} + b_{jk}W_{ik}),\end{aligned}$$

where

$$C_1 = 1.7, \quad C_1^* = 1.80, \quad C_2 = 4.2, \quad C_3 = \tfrac{4}{5}, \quad C_3^* = 1.30, \quad C_4 = 1.25$$
$$C_5 = 0.40, \quad \mathrm{II}_b = b_{ij}b_{ij}.$$

REFERENCES

Abid, R. & Speziale, C. G. 1993 Predicting equilibrium states with Reynolds stress closures in channel flow and homogeneous shear flow. *Phys. Fluids* A **5**, 1776.

Antonia, R. A., Djenidi, L. & Spalart, P. R. 1994*a* Anisotropy of the dissipation tensor in a turbulent boundary layer. *Phys. Fluids* A **6**, 2475.

Antonia, R. A., Spalart, P. R. & Mariani, P. 1994*b* Effect of suction on the near wall anisotropy of a turbulent boundary layer. *Phys. Fluids* A **6**, 430.

Bardina, J., Ferziger, J. H. & Reynolds, W. C. 1983 Improved turbulence models based on large eddy simulations of homogeneous incompressible turbulent flows. *Dept Mech. Engng Tech. Rep.* TF-19. Stanford University.

BERTOGLIO, J. 1982 Homogeneous turbulent field within a rotating frame. *AIAA J.* **20**, 1175.

CHAMPAGNE, F. H., HARRIS, V. G. & CORRSIN, S. 1970 Experiments on nearly homogeneous turbulent shear flow. *J. Fluid Mech.* **41**, 81.

FU, S., LAUNDER, B. E. & TSELEPIDAKIS, D. P. 1987 Accommodating the effects of high strain rates in modeling the pressure strain correlation. *UMIST Mech. Engng Dept Rep.* TFD/87/5.

HAWORTH, D. C. & POPE, S. B. 1986 A generalized Langevin model for turbulent flows. *Phys. Fluids* **29**, 387.

HOLLOWAY, A. G. L. & TAVOULARIS, S. 1992 The effects of curvature on sheared turbulence. *J. Fluid Mech.* **237**, 569.

HOPFINGER, E. J., BROWAND, F. K. & GAGNE, Y. 1982 Turbulence and waves in a rotating tank. *J. Fluid Mech.* **52**, 609.

KIM, J., MOIN, P. & MOSER, R. 1987 Turbulence statistics in the fully developed channel flow at low Reynolds number. *J. Fluid Mech.* **177**, 133.

LAUFER, J. 1951 Investigations of turbulent flow in a two-dimensional channel. *NACA Tech. Rep.* 1053

LAUNDER, B. E., REECE, G. J. & RODI, W. 1975 Progress in the development of a Reynolds-stress turbulence closure. *J. Fluid Mech.* **68**, 537.

LEE, M. J. & REYNOLDS, W. C. 1985 Numerical experiments on the structure of homogeneous turbulence. *Stanford University Tech. Rep.* TF-24.

LESIEUR, M. 1991 *Turbulence in Fluids.* Kluwer.

LUMLEY, J. L. 1967 Rational approach to relations between motions of differing scales in turbulent flows. *Phys. Fluids* **10**, 1405.

LUMLEY, J. L. 1970 Towards a turbulence constitutive relationship. *J. Fluid Mech.* **41**, 413.

MÉTAIS, O. & HERRING, J. R. 1989 Numerical simulation of freely evolving turbulence in stably stratified fluids. *J. Fluid Mech.* **202**, 117.

POPE, S. B. 1983 Consistent modeling of scalars in turbulent flow. *Phys. Fluids* **26**, 404.

REYNOLDS, W. C. 1989 Effect of rotation on homogeneous turbulence. *10th Australasian Fluid Mechanics Conf., Melbourne, Australia.*

REYNOLDS, W. C. 1994 Fundamentals of turbulence for turbulence modeling and simulation. *Stanford Class Notes.*

REYNOLDS, W. C. & KASSINOS, S. C. 1994 A one-point model for the evolution of the Reynolds stress and structure tensors in rapidly deformed homogeneous turbulence. *Osborne Reynolds Centenary Symposium. UMIST, Manchester, UK.*

RISTORCELLI, J. R. 1987 A realizable rapid-pressure model satisfying two-dimensional frame-indifference and valid for three-dimensional three-component turbulence. *Sibley School of Mech. and Aerospace Engng Rep.* FDA-87-19. Cornell University.

RISTORCELLI, J. R. 1991 Second-order turbulence simulation of the rotating, buoyant, recirculating convection in the Czochralski crystal melt. *Sibley School of Mech. and Aerospace Engng Rep.* FDA-91-14; PhD Thesis, Cornell University.

RISTORCELLI, J. R. & LUMLEY, J. L. 1991*a* Turbulence simulations of the Czochralski crystal melt: Part 1 – the buoyantly driven flow. *Sibley School of Mech. and Aerospace Engng Rep.* FDA-91-04. Cornell University.

RISTORCELLI, J. R. & LUMLEY, J. L. 1991*b* Synopsis of a rapid-pressure model materially frame indifferent in the 2D limit. *Sibley School of Mech. and Aerospace Engng Rep.* FDA-91-15. Cornell University

RISTORCELLI, J. R. & LUMLEY, J. L. 1993 A second-order simulation of the Czochralski crystal growth melt: the buoyantly driven flow. *J. Cryst. Growth* **129**, 249–265.

RIVLIN, R. S. 1955 Further remarks on the stress deformation relations for isotropic materials. *Arch. Rat. Mech. Anal.* **4**, 681.

ROGERS, M. M., MOIN, P. & REYNOLDS, W. C. 1986 The structure and modeling of the hydrodynamic and passive scalar fields in homogeneous turbulent shear flow. *Dept Mech. Engng Tech. Rep.* TF-25. Stanford University.

SHIH, T. H. & LUMLEY, J. L. 1985 Modeling of pressure correlation terms in Reynolds stress and scalar flux equations. *Sibley School Mech. and Aerospace Engng Rep.* FDA-85-3. Cornell University.

SMITH, G. F. 1971 On isotropic functions of symmetric tensors, skew symmetric tensors and vectors. *Intl. J. Engng Sci.* **9**, 899.

SPENCER, A. J. M. 1971 Theory of invariants. In *Continuum Physics* (ed. A. C. Eringen), vol. 1, p. 240. Academic.

SPEZIALE, C. G. 1981 Some interesting properties of two-dimensional turbulence. *Phys. Fluids* **24**, 1425.

SPEZIALE, C. G. 1985 Second-order closure models for rotating turbulent flows. *ICASE Rep.* 85-49. NASA-Langley, Hampton, VA.

SPEZIALE, C. G. 1989 Turbulence modeling in noninertial frames of reference. *Theoret. Comput. Fluid Dyn.* **1**, 3.

SPEZIALE, C. G., ABID, R. & DURBIN, P. A. 1994 On the realizability of Reynolds stress closures turbulence closures. *J. Sci. Comput.* **9**, 369.

SPEZIALE, C. G., GATSKI, T. B. & SARKAR, S. 1992 On testing models for the pressure-strain correlation of turbulence using direct simulations. *Phys. Fluids* A **4**, 2887.

SPEZIALE, C. G. & MHUIRIS, N. M. G. 1989*a* Scaling laws for homogeneous turbulent shear flows in rotating frames. *Phys. Fluids* A **1**, 294.

SPEZIALE, C. G. & MHUIRIS, N. M. G. 1989*b* On the prediction of equilibrium states in homogeneous turbulence. *J. Fluid Mech.* **209**, 591.

SPEZIALE, C. G., SARKAR, S. & GATSKI, T. B. 1991 Modelling the pressure–strain correlation of turbulence – an invariant dynamical systems approach. *J. Fluid Mech.* **227**, 245.

TAVOULARIS, S. & CORRSIN, S. 1981 Experiments in nearly homogeneous turbulent shear flows with a uniform mean temperature gradient. Part 1. *J. Fluid Mech.* **104**, 369.

TAVOULARIS, S. & KARNIK, U. 1989 Further experiments on the evolution of turbulent stresses and scales in uniformly sheared turbulence. *J. Fluid Mech.* **204**, 457.